



Bulk physics: critical point search

Lijuan Ruan (BNL)
September 3rd, 2023

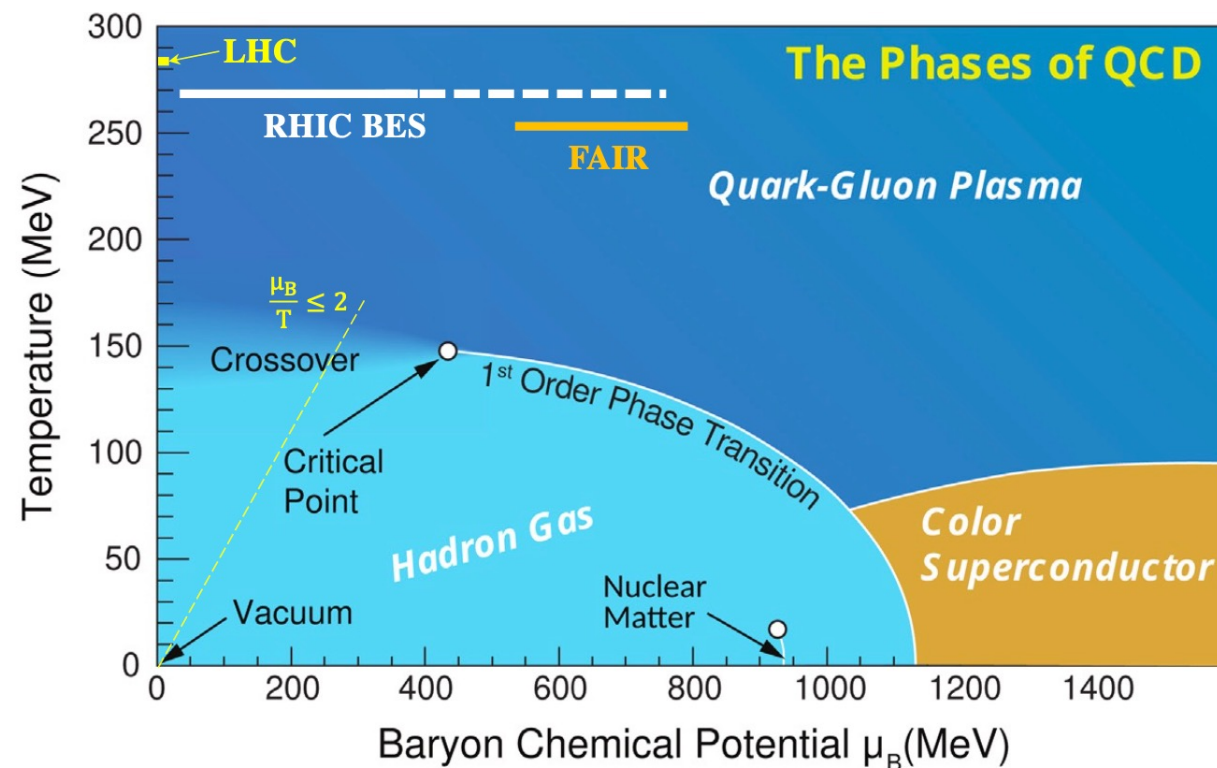


The phases of QCD matter

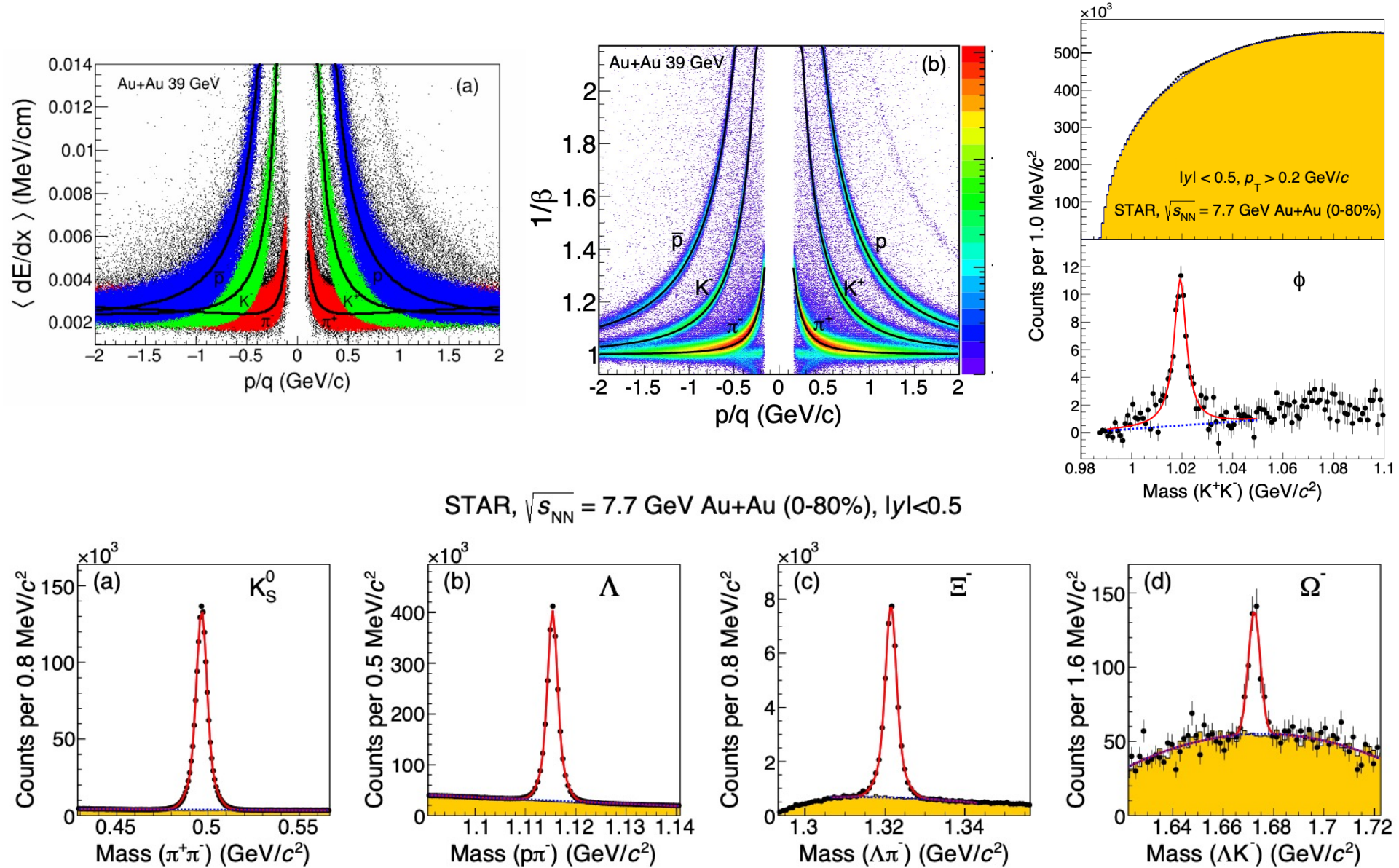
Lattice QCD: crossover chiral transition at $\mu_B < 2 T$

At top RHIC and LHC energies, measurements consistent with a smooth crossover chiral transition

Change T and μ_B by varying the collision energy.

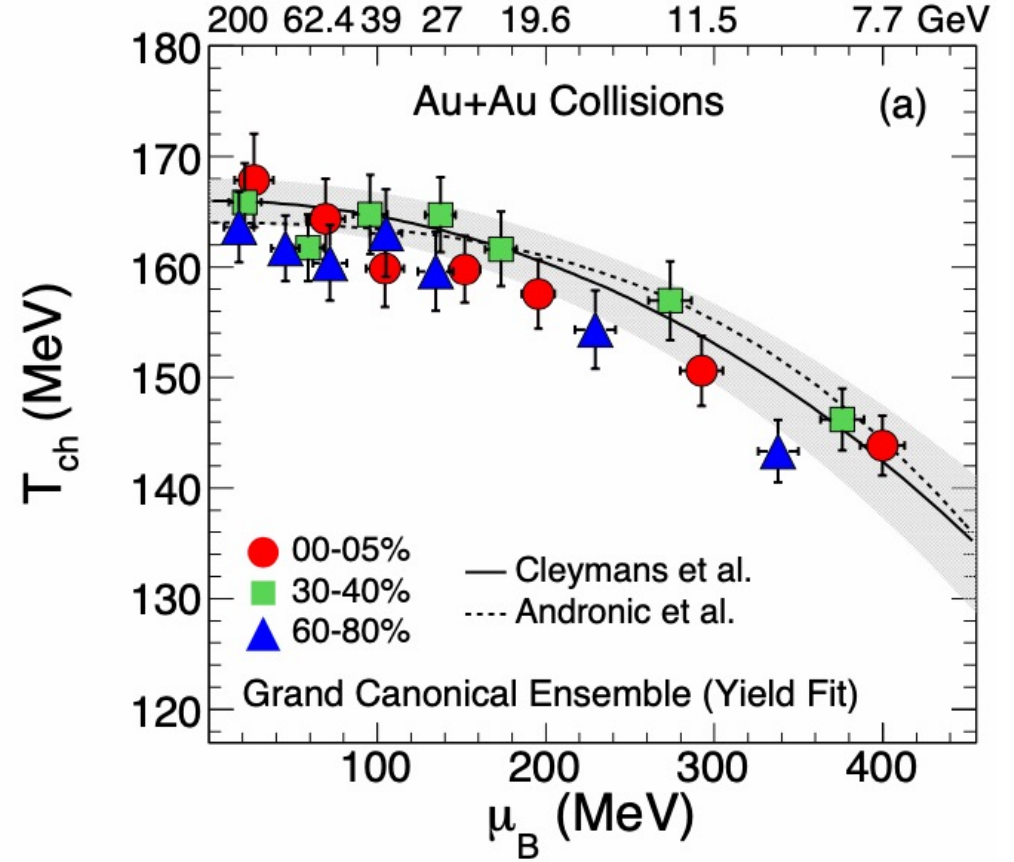
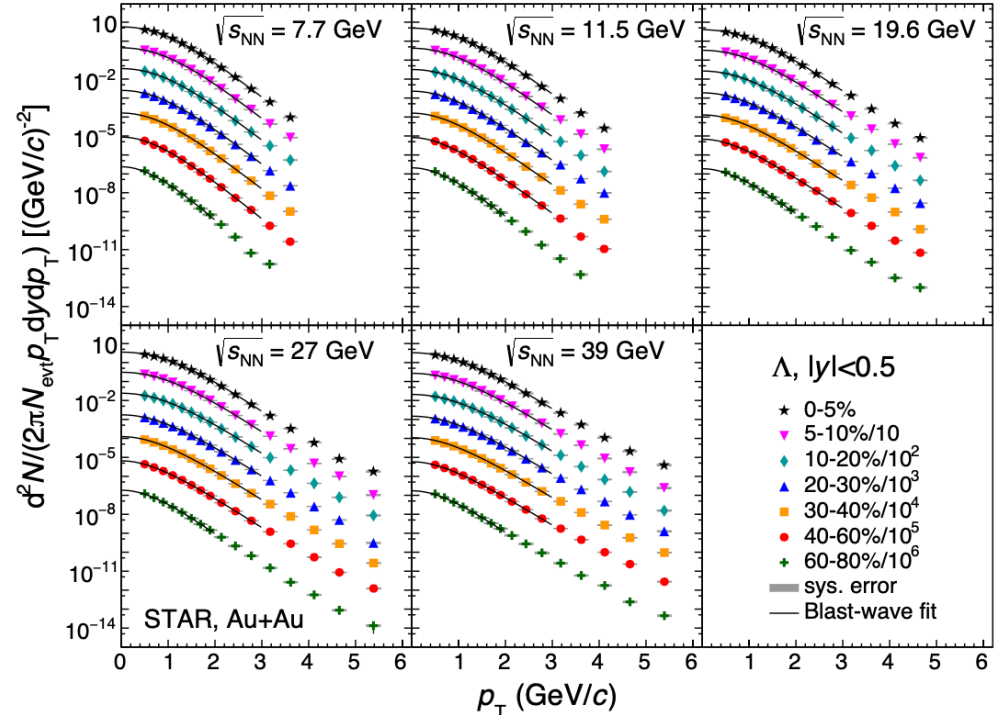
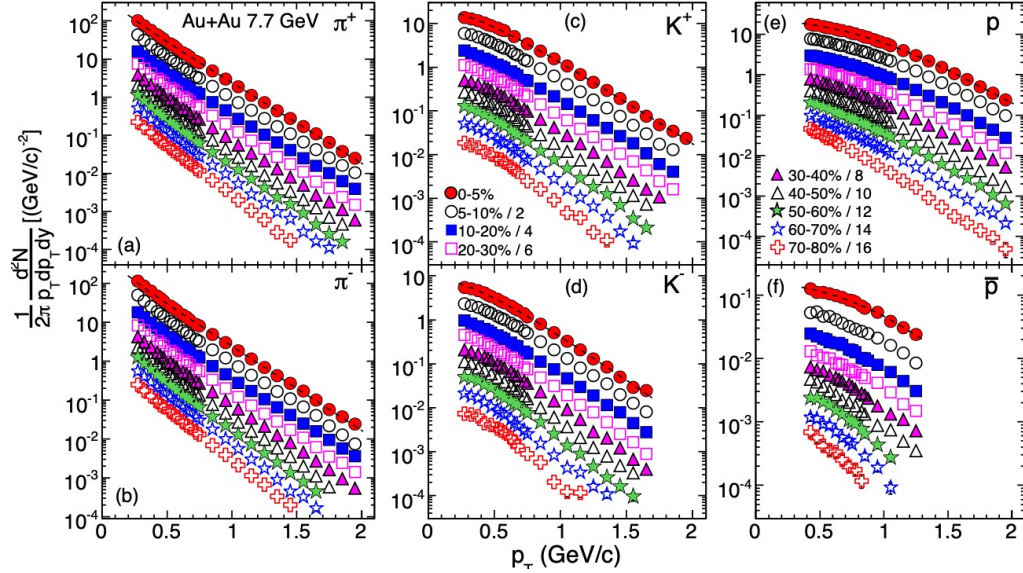


What do we need to measure T and μ_B



What do we need to measure T and μ_B

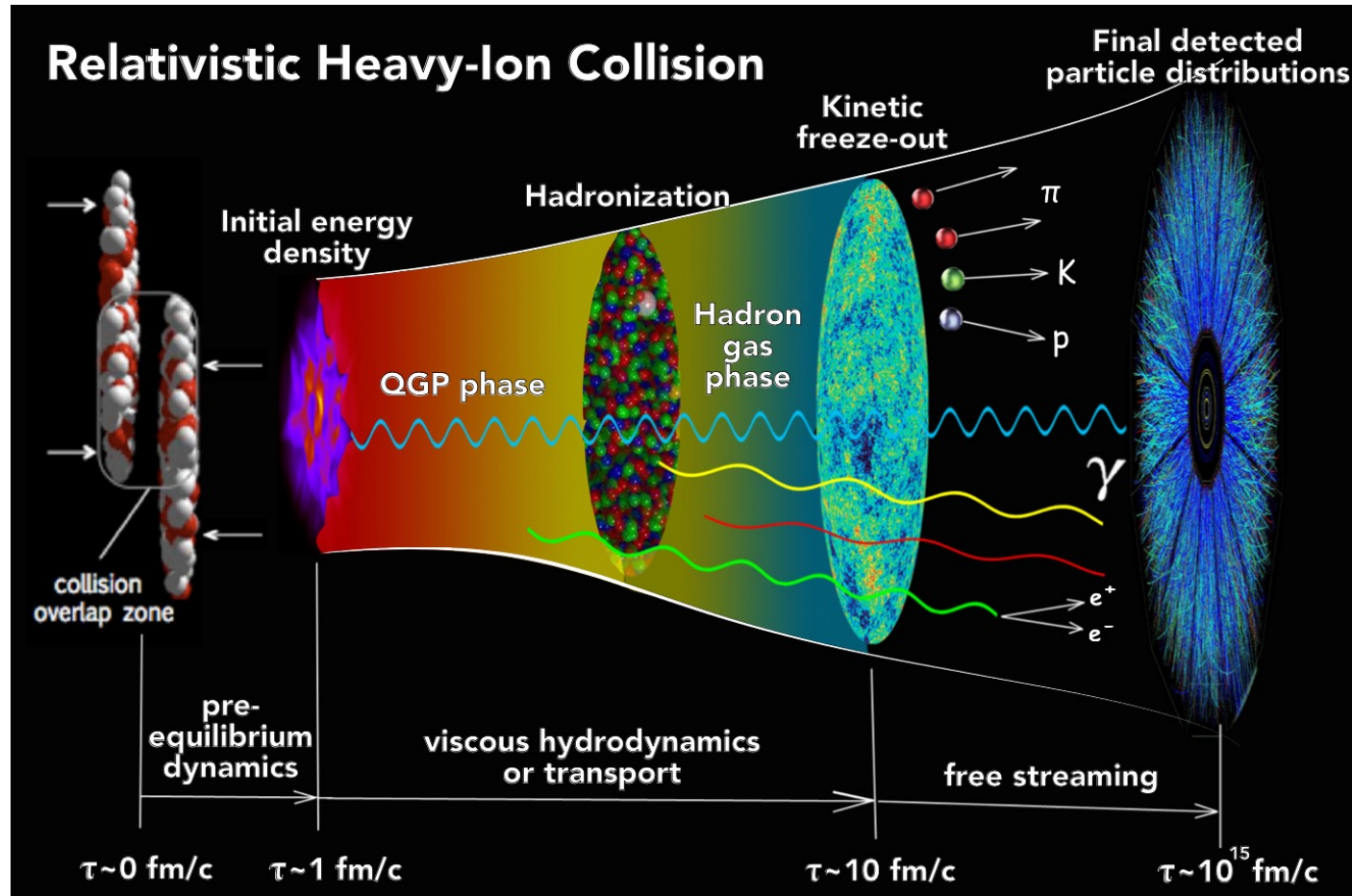
Phys. Rev. C 96 (2017) 44904



$\pi^\pm, K^\pm, p, \bar{p}, \Lambda, \bar{\Lambda}, \Xi, \text{ and } \bar{\Xi}.$

$\pi^-/\pi^+, \bar{K}^-/K^+, \bar{p}/p, \bar{\Lambda}/\Lambda, \bar{\Xi}/\Xi, K^-/\pi^-, \bar{p}/\pi^-, \Lambda/\pi^-,$
and $\bar{\Xi}/\pi^-.$

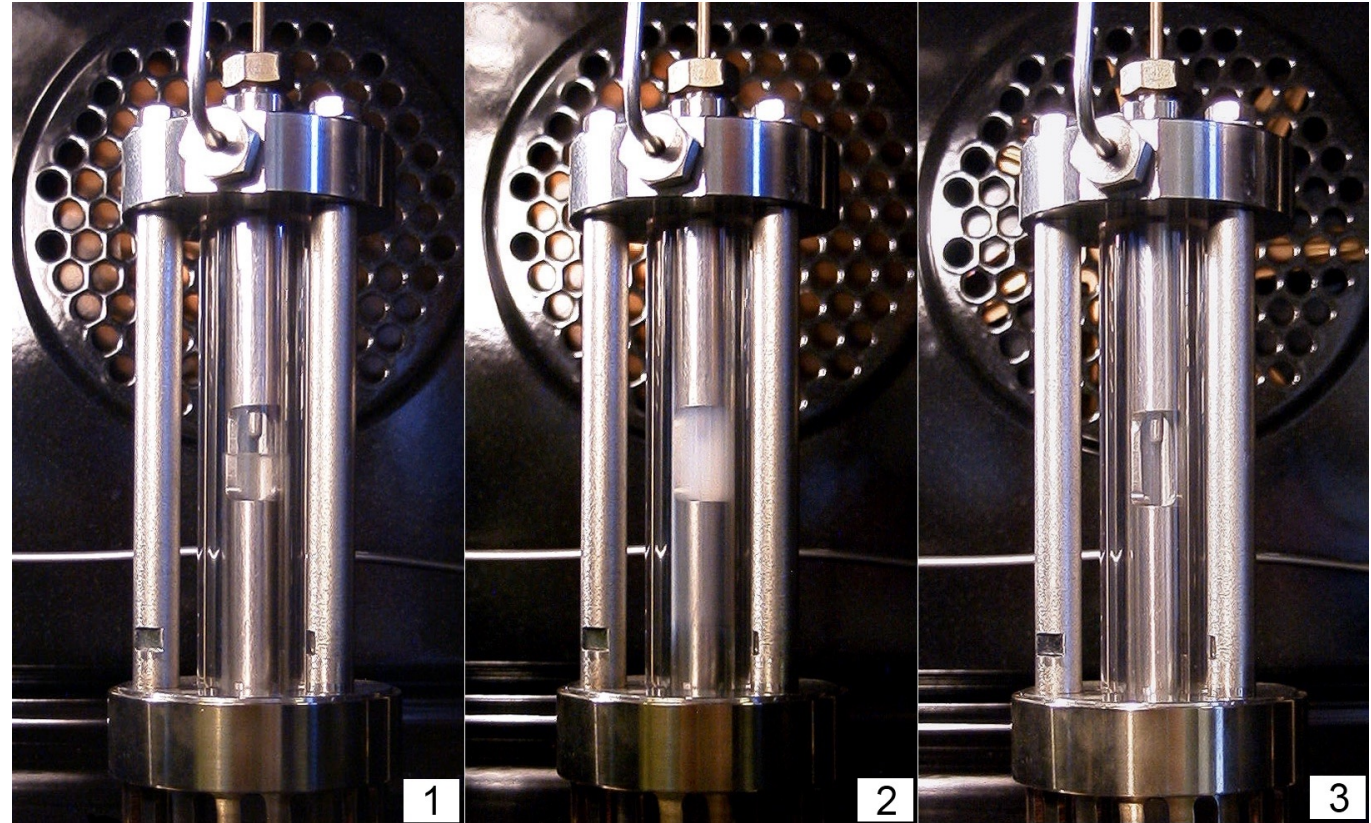
The system is dynamic



How to infer the QCD critical point

Divergence of the correlation length, dynamics slow down, Large density fluctuations

Critical opalescence, magnetic susceptibility



How to infer the QCD critical point

Correlation length related to various moments of the distributions of conserved quantities such as net-baryon, net-charge, and net-strangeness.

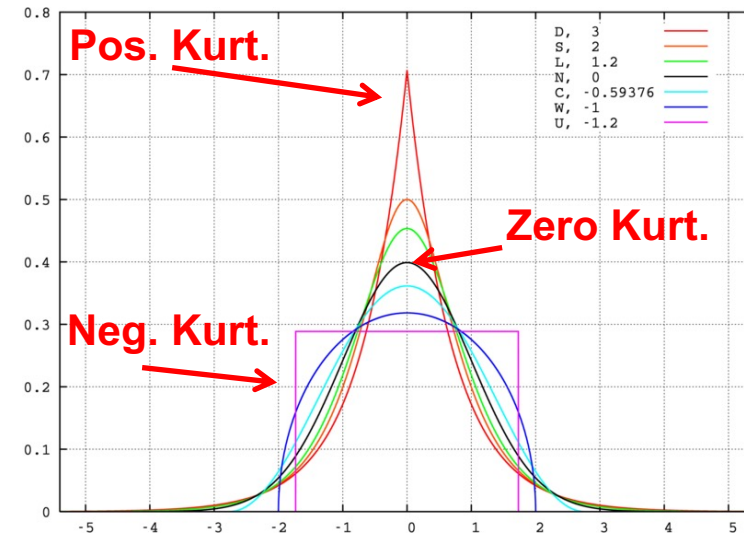
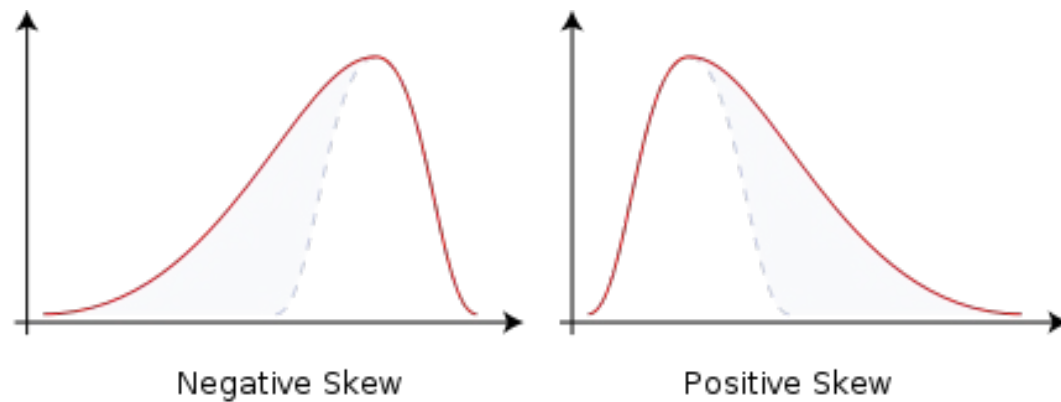
$$\langle (\delta N)^2 \rangle \approx \xi^2, \langle (\delta N)^3 \rangle \approx \xi^{4.5}, \langle (\delta N)^4 \rangle - 3 \langle (\delta N)^2 \rangle^2 \approx \xi^7$$

Mean: $M = \langle N \rangle$

St. Deviation: $\sigma = \sqrt{\langle (N - \langle N \rangle)^2 \rangle}$

Skewness: $S = \frac{\langle (N - \langle N \rangle)^3 \rangle}{\sigma^3}$

Kurtosis: $\kappa = \frac{\langle (N - \langle N \rangle)^4 \rangle}{\sigma^4} - 3$



Measure non-Gaussian fluctuation of conserved quantities

Connection to Lattice QCD

Lattice calculations show that moments of the conserved charge (net-baryon, net-charge, net-strangeness) distributions are related to the susceptibilities

Pressure:

$$\frac{p}{T^4} = \frac{1}{VT^3} \ln Z(V, T, \mu_B, \mu_Q, \mu_S)$$

Susceptibility:

$$\chi_q^{(n)} = \frac{1}{T^4} \frac{\partial^n}{\partial (\mu_q / T)^n} P \left(\frac{T}{T_c}, \frac{\mu_q}{T} \right) \Big|_{T/T_c},$$

$q = B, Q, S$ **(Conserved Quantum Number)**

$$\chi_q^{(1)} = \frac{1}{VT^3} \langle \delta N_q \rangle, \chi_q^{(2)} = \frac{1}{VT^3} \langle (\delta N_q)^2 \rangle$$

$$\chi_q^{(3)} = \frac{1}{VT^3} \langle (\delta N_q)^3 \rangle$$

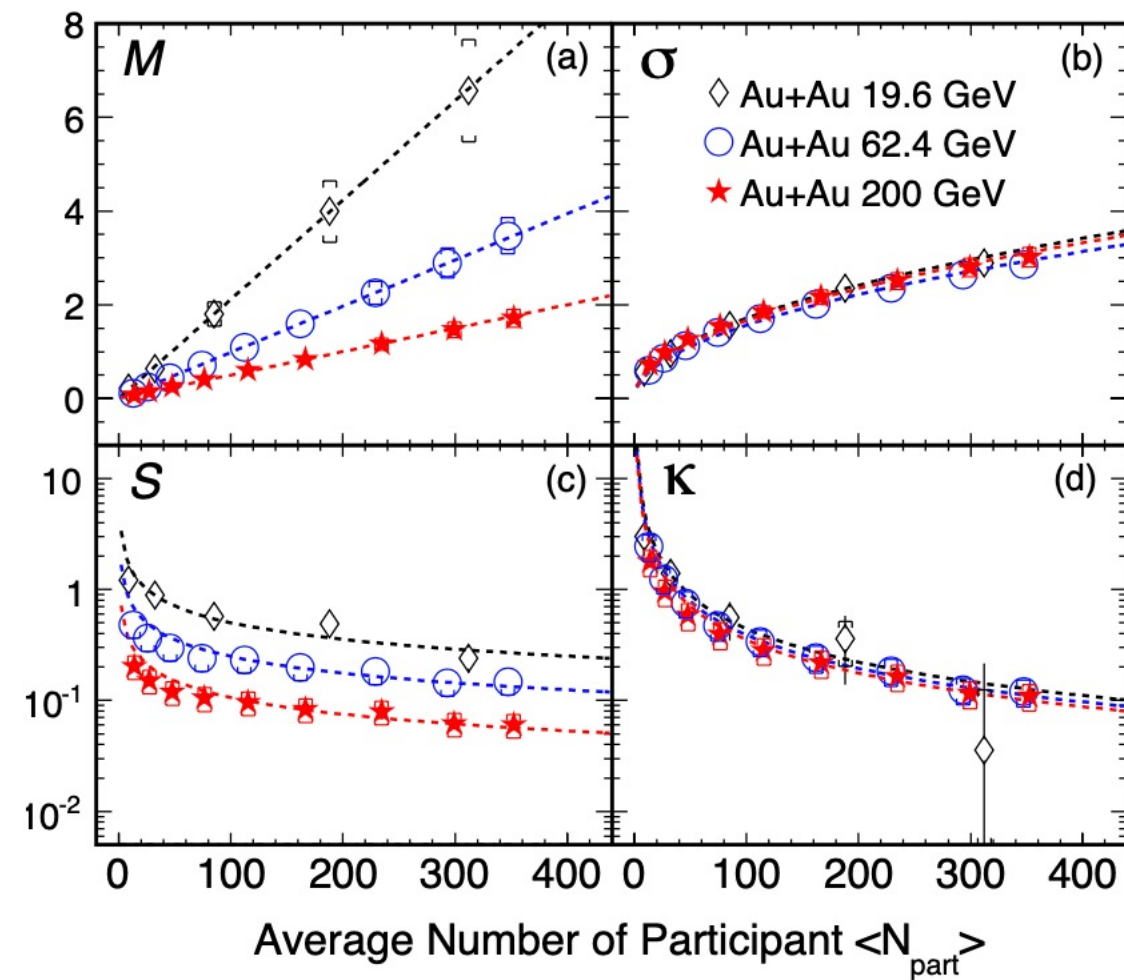
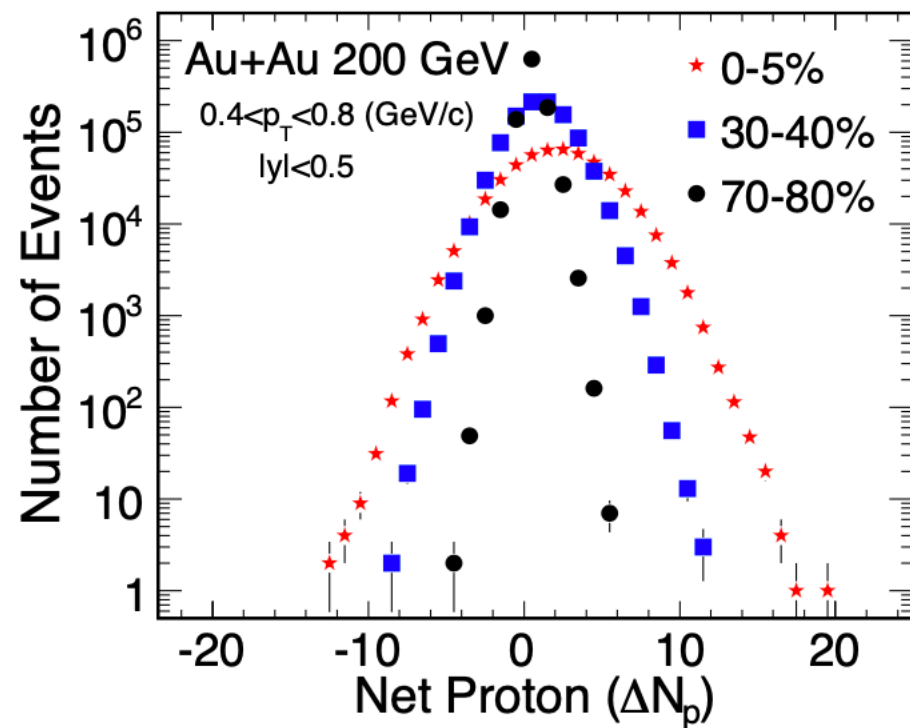
$$\chi_q^{(4)} = \frac{1}{VT^3} \left(\langle (\delta N_q)^4 \rangle - 3 \langle (\delta N_q)^2 \rangle^2 \right)$$

A. Bazavov et al *arXiv*:1208.1220, 1207.0784.

F. Karsch et al, PLB 695, 136 (2011).

arXiv: 1203.0784; S. Borsanyi et al, JHEP1201,138(2011);

High moments of net-proton multiplicity distributions

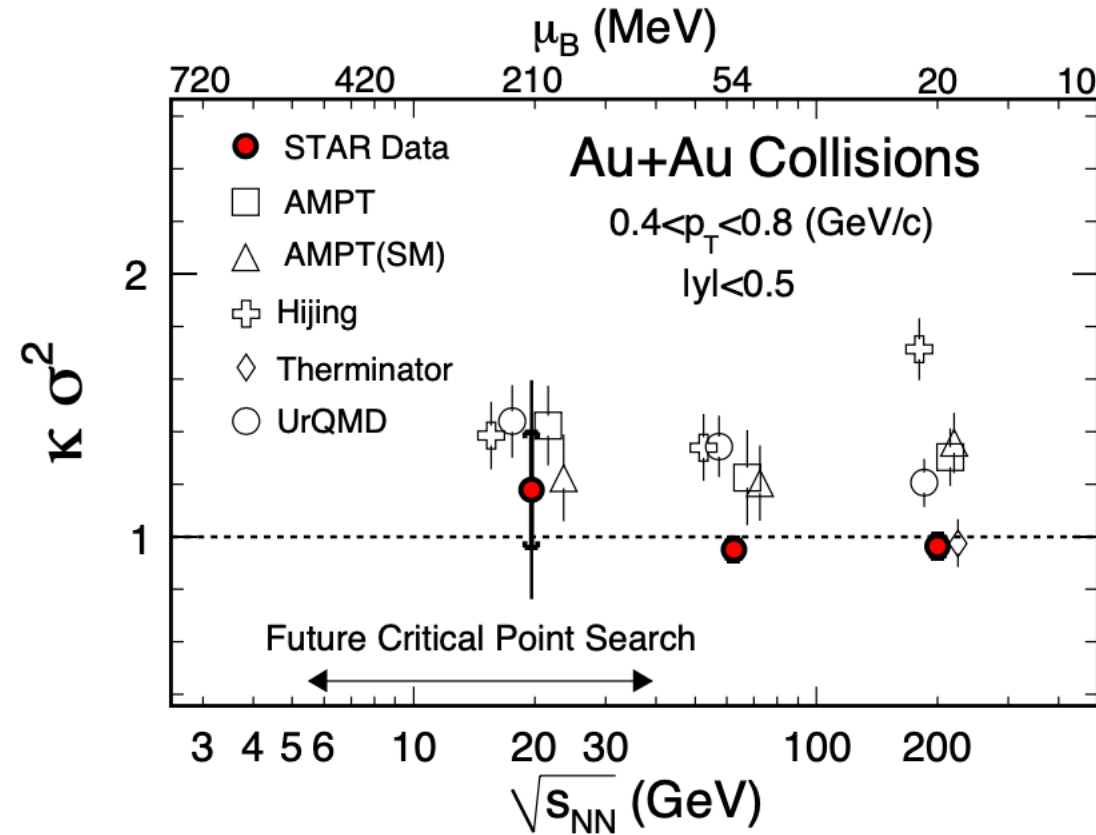


$$K\sigma^2 \sim \frac{\chi^{(4)}}{\chi^{(2)}}, S\sigma \sim \frac{\chi^{(3)}}{\chi^{(2)}}, \frac{\sigma^2}{M} \sim \frac{\chi^{(2)}}{\chi^{(1)}}$$

PRL 105 (2010) 022302

High moments of net-proton multiplicity distributions

PRL 105 (2010) 022302



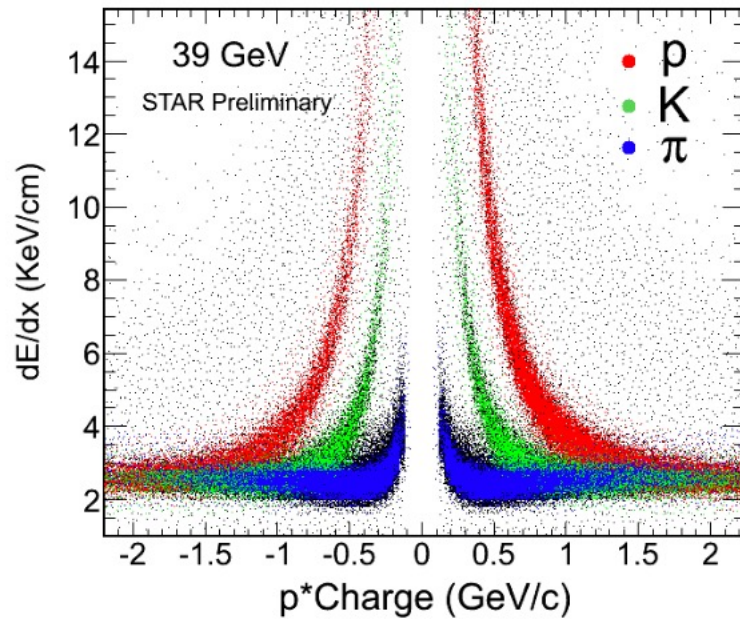
No evidence for a QCD critical point in the QGP phase diagram for $\mu_B < 200$ MeV

0.04 M, 5 M, 8 M data used for 19.6, 62.4, and 200 GeV respectively.

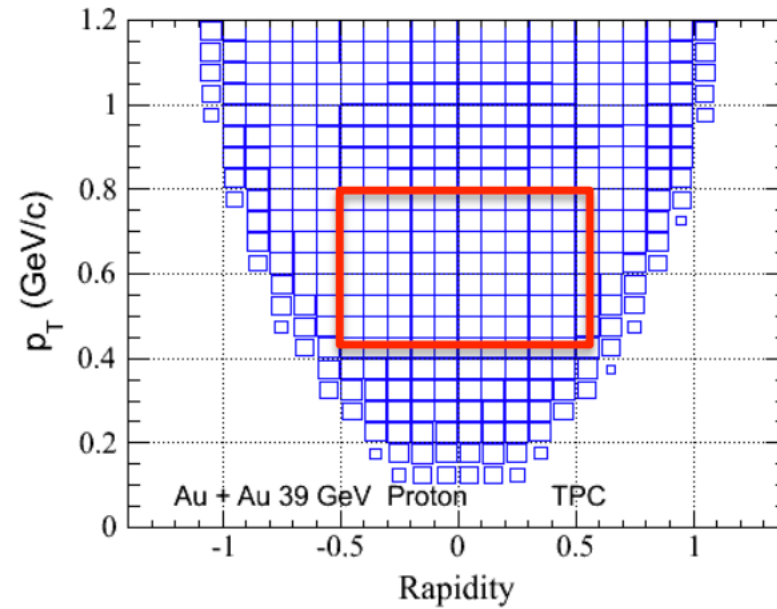
Go to STAR Beam Energy Scan Phase I (BES-I)

Energy (GeV)	7.7	11.5	19.6	27	39	62.4	200
Statistics (Million)	~3	~6.6	~15	~30	~87	~47	~242
Year	2010	2010	2011	2011	2010	2010	2010

STAR TPC dE/dx PID



Proton Phase Space



Net-proton higher moments from BES-I

$20 < \mu_B < 420 \text{ MeV}$

UrQMD includes baryon conservation and hadronic scattering effects

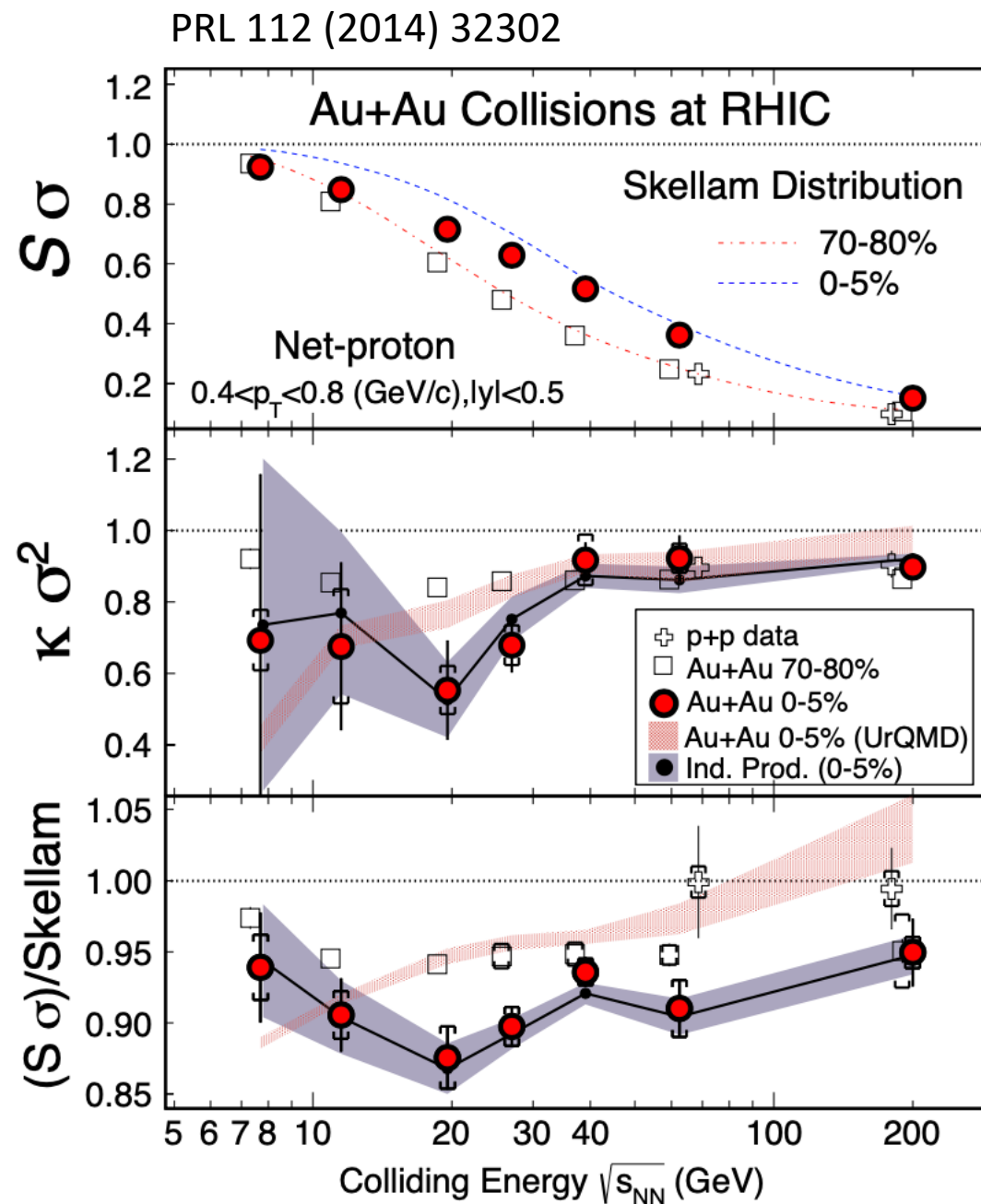
At $\sqrt{s_{NN}} > 39 \text{ GeV}$, results from p+p, peripheral, and central Au+Au similar

Deviate from Skellam and UrQMD expectations at $\sqrt{s_{NN}} \leq 27 \text{ GeV}$

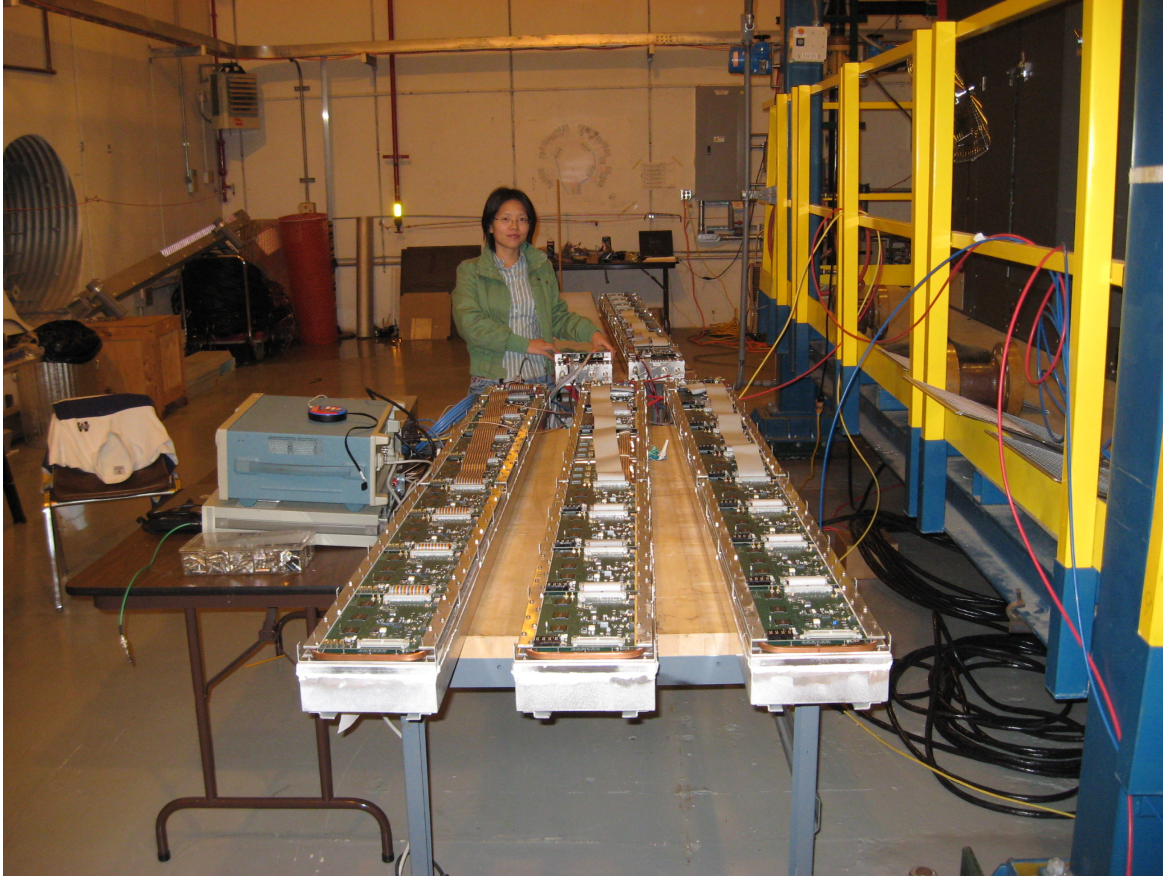
Data reasonably described by assuming independent production of proton and anti-proton

Comprehensive analysis techniques developed including centrality bin width correction, statistical error estimation (Delta theorem method, centrality resolution effect etc.)

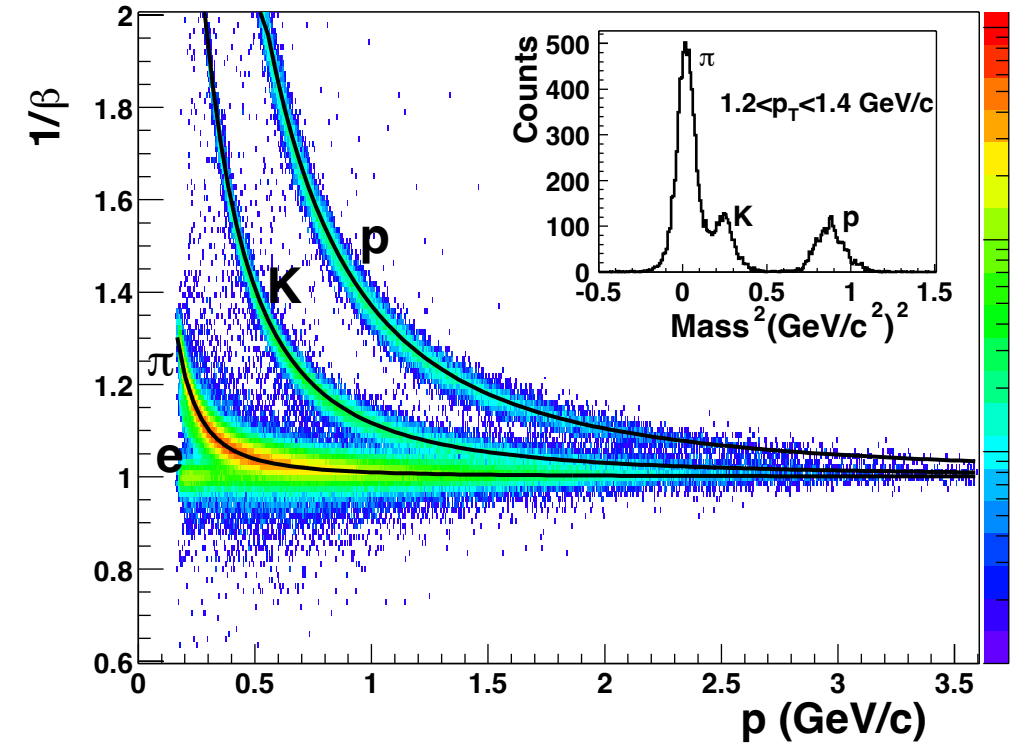
STAR full time of flight detector was installed for Run 2010 and beyond



STAR Time of Flight detector upgrade



US-China Collaboration, 120 units in total:
2008: 4%; 2009: 72%; 2010: 100%



STAR Collaboration, PLB616(2005)8

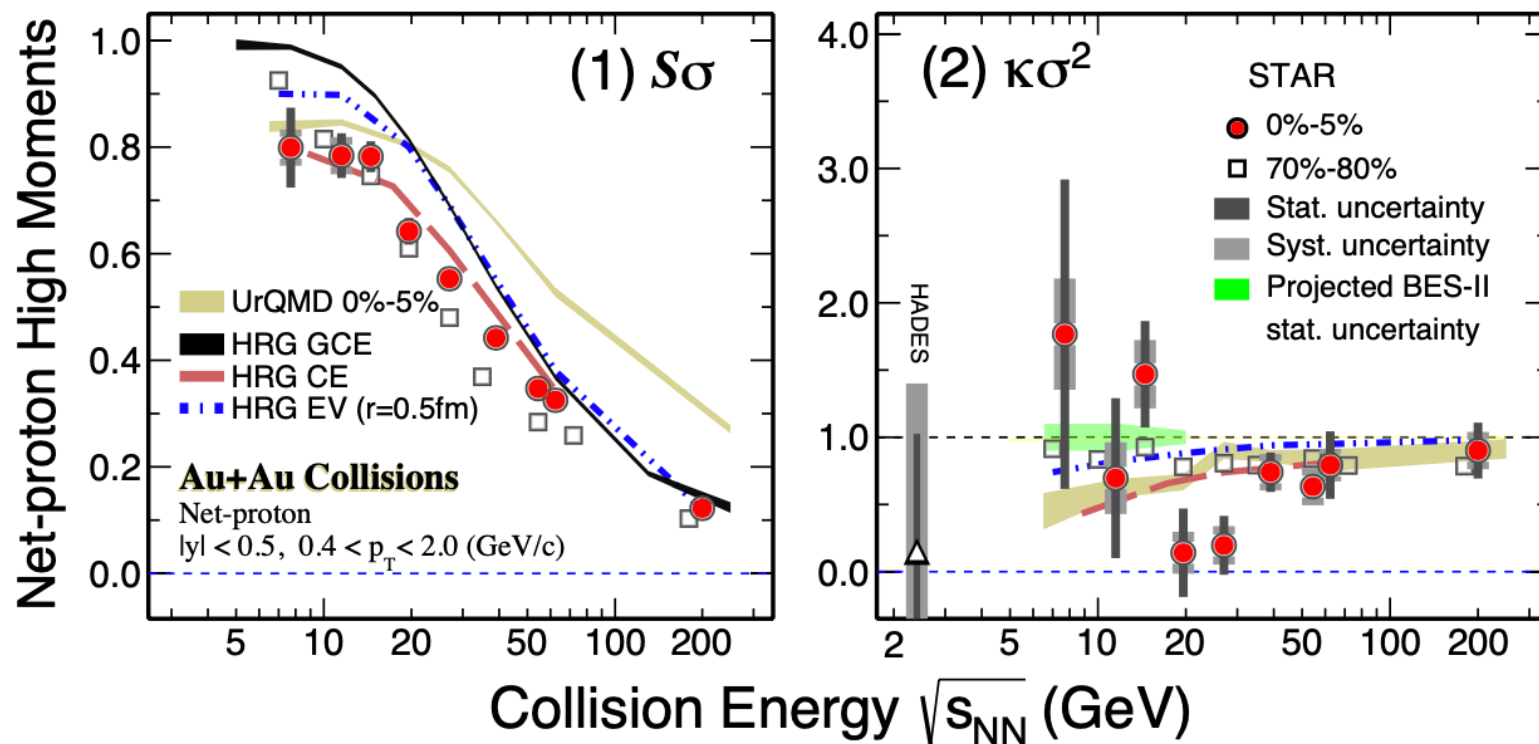
Net-proton higher moments from BES-I with TOF

PRL 126 (2021) 92301

$20 < \mu_B < 420 \text{ MeV}$

p_T range extended to 0.4-2 GeV/c

14.5 and 54.4 GeV data included



First evidence of a non-monotonic variation in kurtosis times variance of the net-proton number distribution as a function of collision energy with 3.1 sigma significance

STAR BES-II upgrades

Major improvements for
BES-II

iTPC Upgrade:

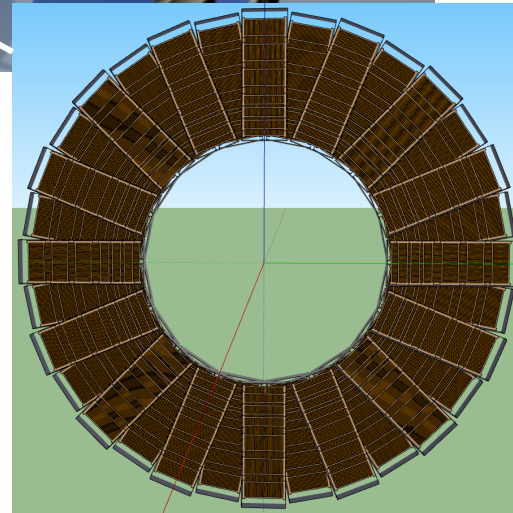
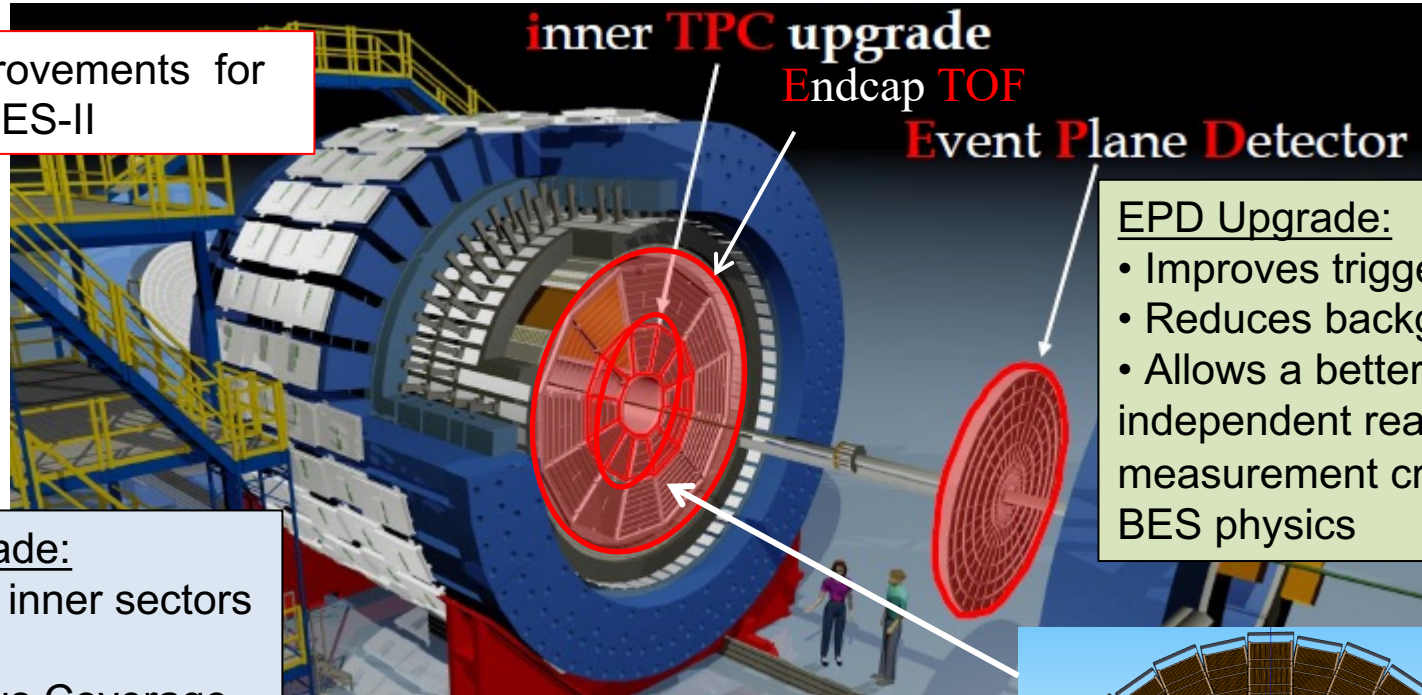
- Replaced inner sectors of the TPC
- Continuous Coverage
- Improves dE/dx
- Extends η coverage from 1.0 to 1.5
- Lowers p_T cut from 125 MeV/c to 60 MeV/c

EndCap TOF Upgrade:

- Rapidity coverage is critical
- PID at $\eta = 1$ to 1.5
- Improves the fixed target program
- Provided by CBM-FAIR

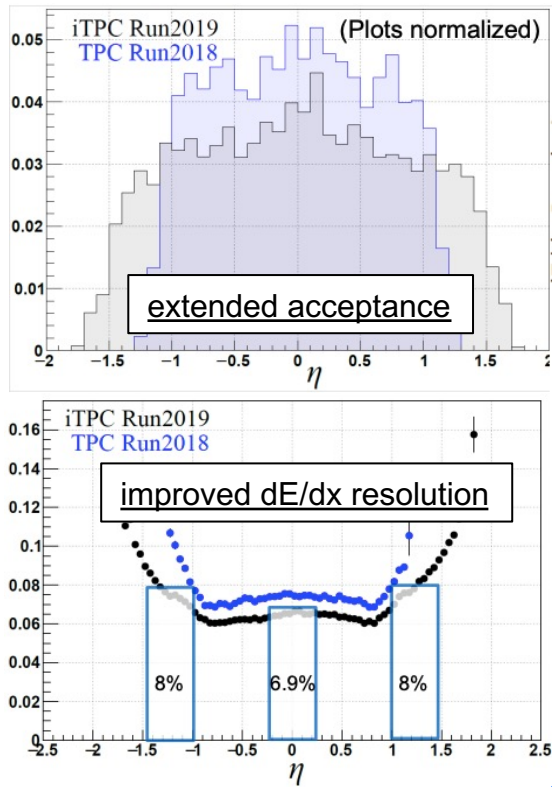
EPD Upgrade:

- Improves trigger
- Reduces background
- Allows a better and independent reaction plane measurement critical to BES physics

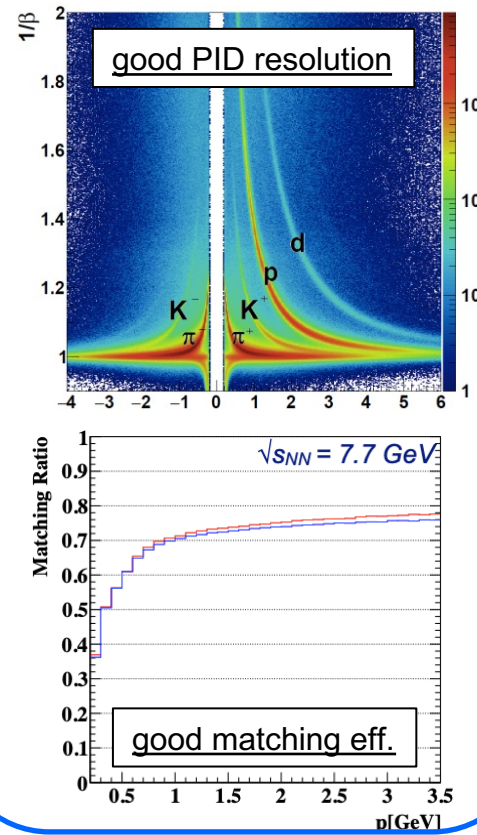


Detector performance

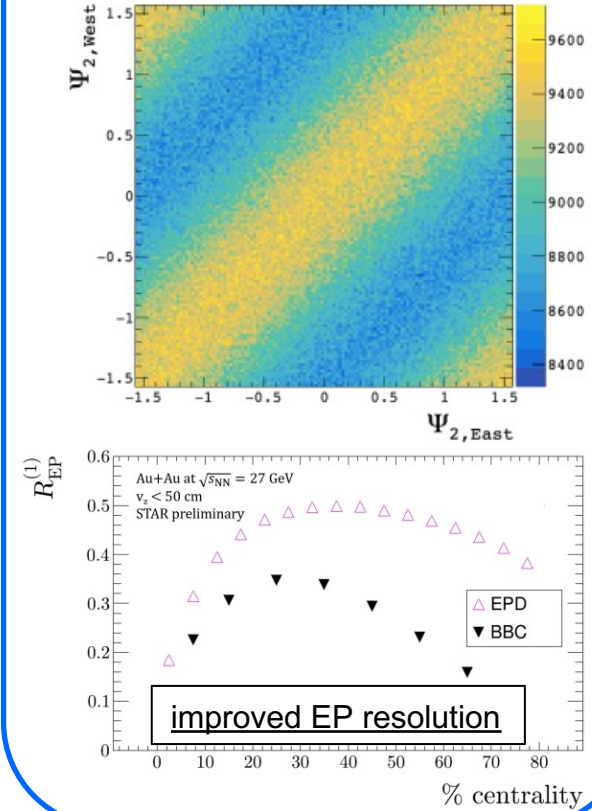
iTPC (2019+)



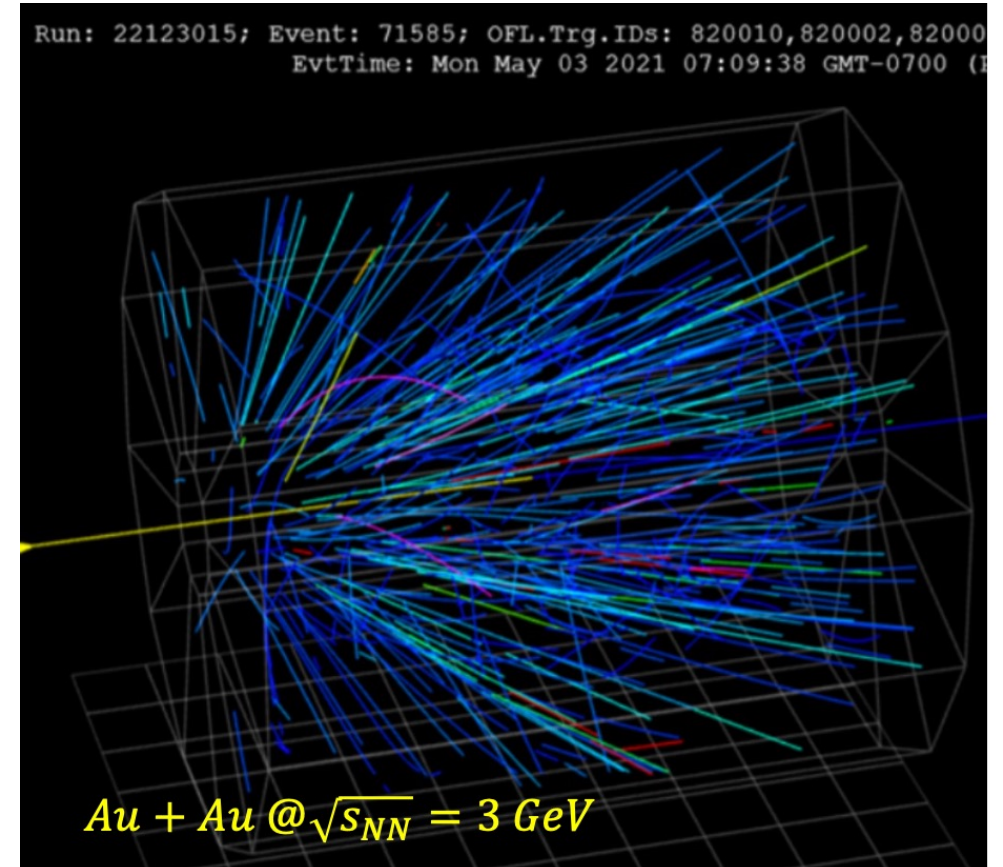
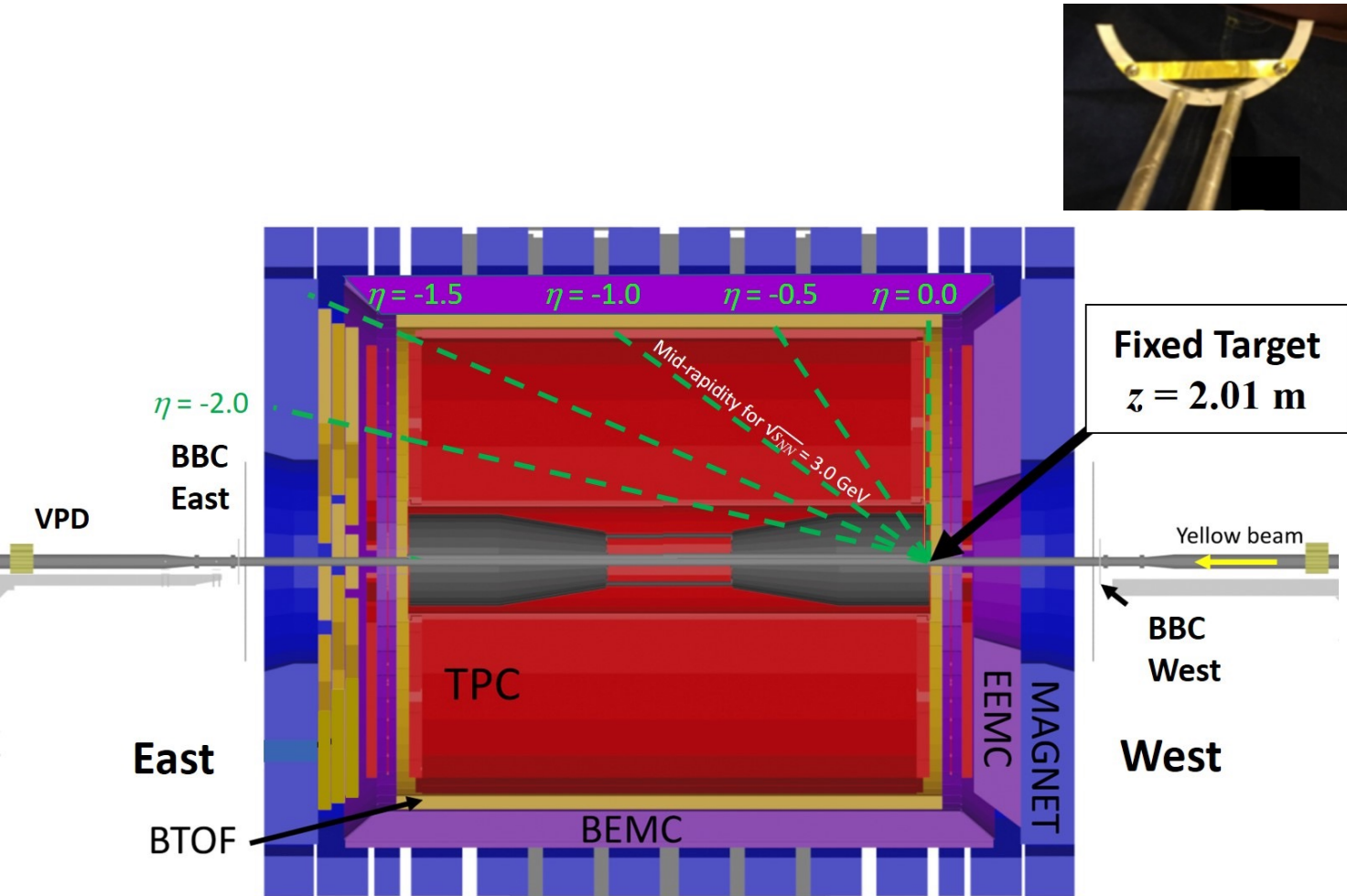
eTOF (2019+)



EPD (2018+)

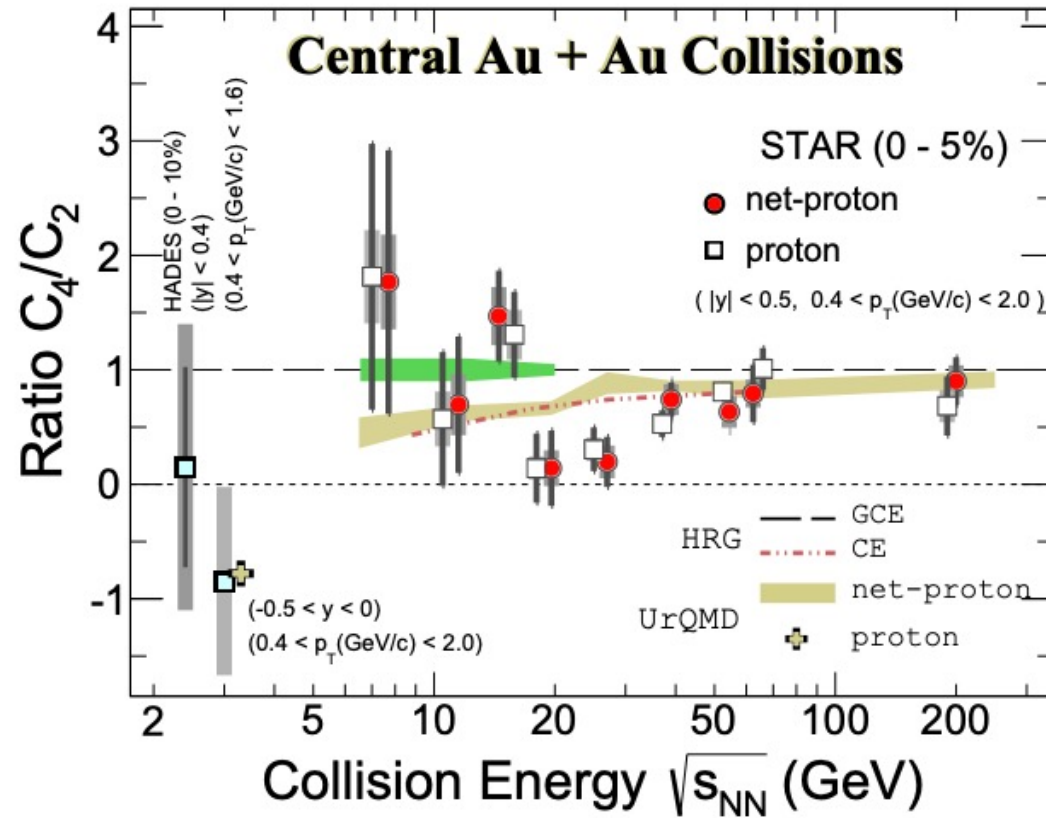


STAR as a fixed-target experiment

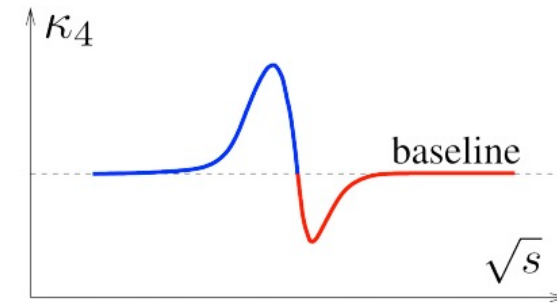


A gold target was installed inside the beam pipe in 2014

Results at 3 GeV from FXT



BES-I: PRL 126 (2021) 092301
3 GeV data: PRL 128 (2022) 202303



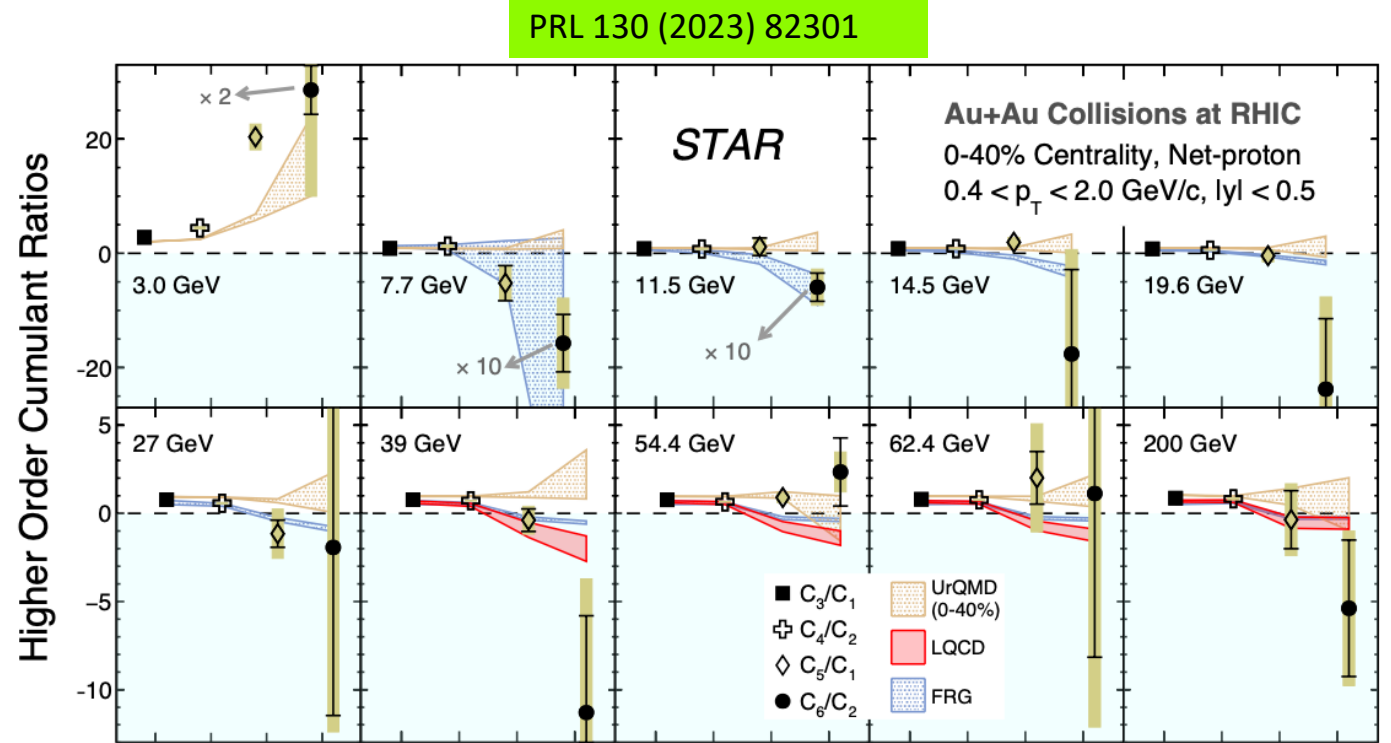
- Non-monotonic energy dependence in central Au+Au collisions (3.1σ)
- Strong suppression in proton C_4/C_2 at 3 GeV
- consistent with UrQMD hadronic transport model calculation

BES-II data collected at RHIC will cover a broad and interesting range of μ_B for the critical point search

Higher order net-proton number fluctuations

Calculations with a cross-over quark-hadron transition (LQCD and FRG) predict a particular ordering of susceptibility ratios:

$$\chi_3^B / \chi_1^B > \chi_4^B / \chi_2^B > \chi_5^B / \chi_1^B > \chi_6^B / \chi_2^B$$



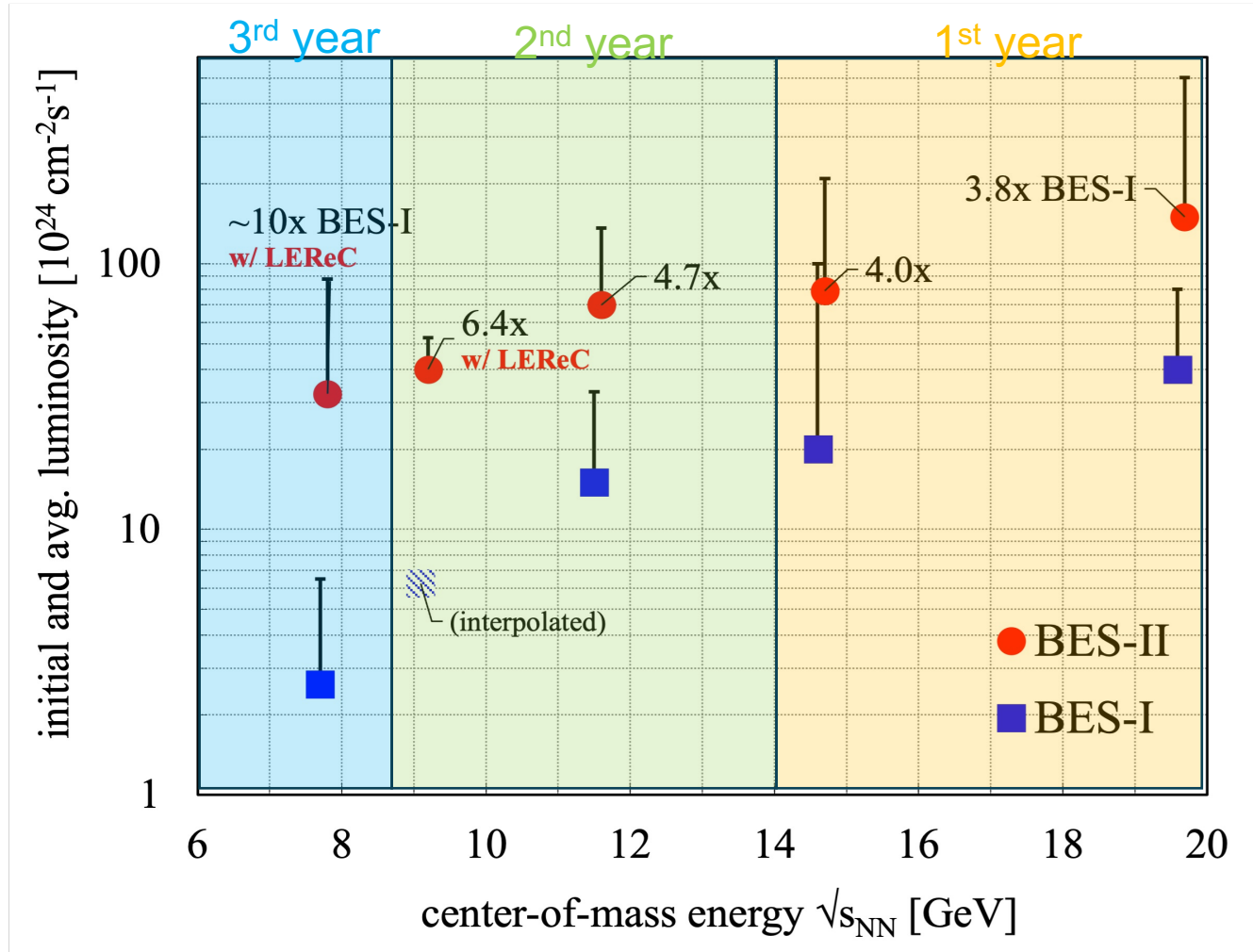
- At 7.7-200 GeV, net-proton cumulant ratios consistent with the ordering predicted by LQCD and FRG:

$$C_3/C_1 > C_4/C_2 > C_5/C_1 > C_6/C_2$$

- The 3 GeV data show a reversing trend

The structure of QCD matter at high baryon density $\mu_B \sim 720$ MeV starkly different from those at vanishing μ_B

Beam energy scan phase II (BES-II) in 2019-2021



Goal was $L_{\text{avg}} (\text{BES-II}) = 4x L_{\text{avg}} (\text{BES-I})$

In BES-II

$3.8 \times L_{\text{avg}} (\text{BES-I})$

$4.0 \times L_{\text{avg}} (\text{BES-I})$

$4.7 \times L_{\text{avg}} (\text{BES-I})$

$6.4 \times L_{\text{avg}} (\text{BES-I})$

$\sim 10 \times L_{\text{avg}} (\text{BES-I})$

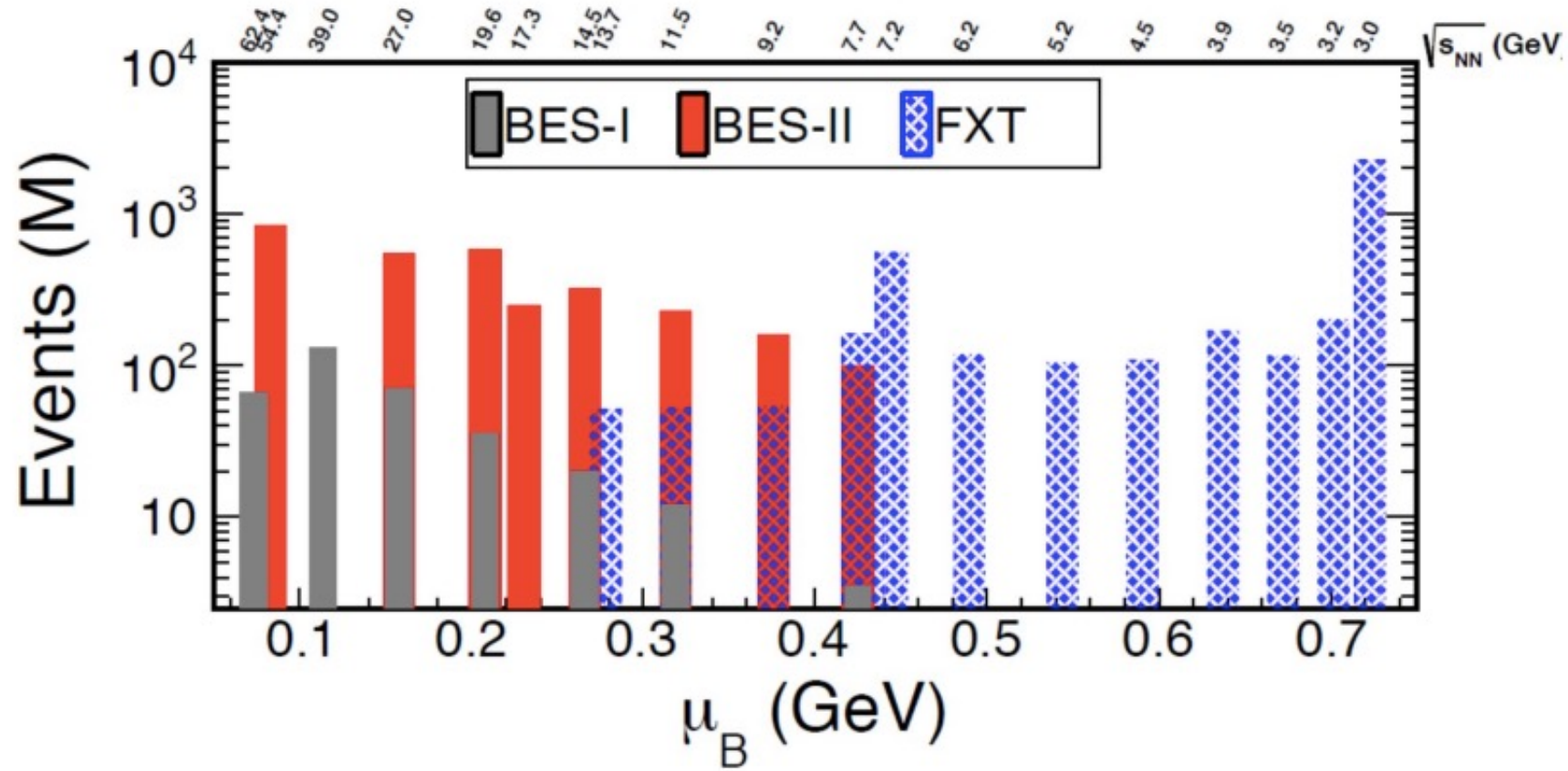
with
LEReC
at lowest
beam
energies

RHIC is unique to map the phase diagram of QCD:

Beam energy scan II: collision energies 7.7, 9.2, 11.5, 14.6, 17.3, 19.6 GeV and 12 fixed-target energies

In 2021, collected the last collider data set at 7.7 GeV, completed the BES-II program.

BES-II datasets

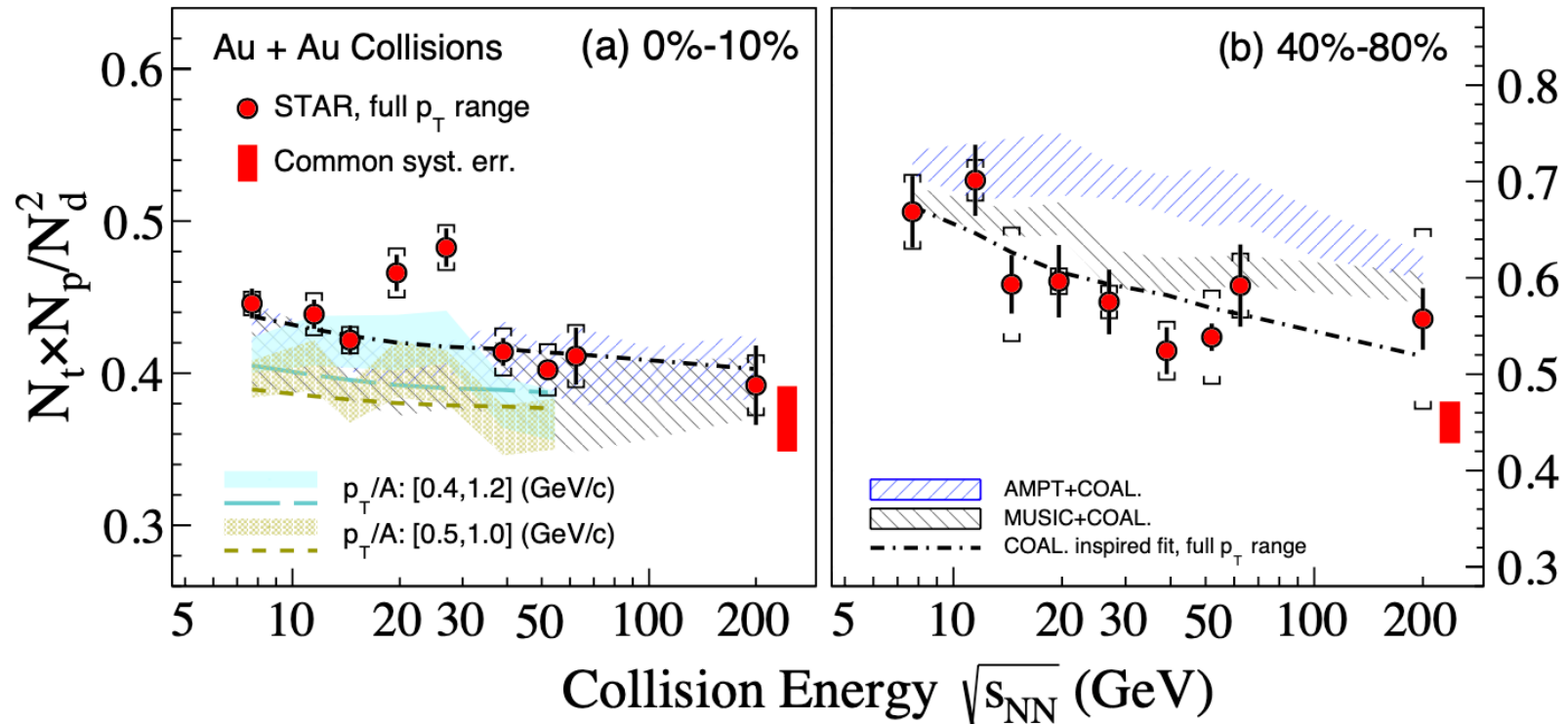


A broad μ_B coverage: $20 < \mu_B < 720$ MeV

Any other measurements?

Light nuclei yield ratio

PRL 130 (2023) 202301



$N_t N_p / N_d^2$, sensitive to fluctuations of the local neutron density shows enhancements relative to the coalescence baseline with a significance of 2.3σ and 3.4σ respectively in 0 –10% central Au+Au collisions at 19.6 and 27 GeV.

Constrain production dynamics of light nuclei and understanding of the QCD phase diagram

Photons and dileptons

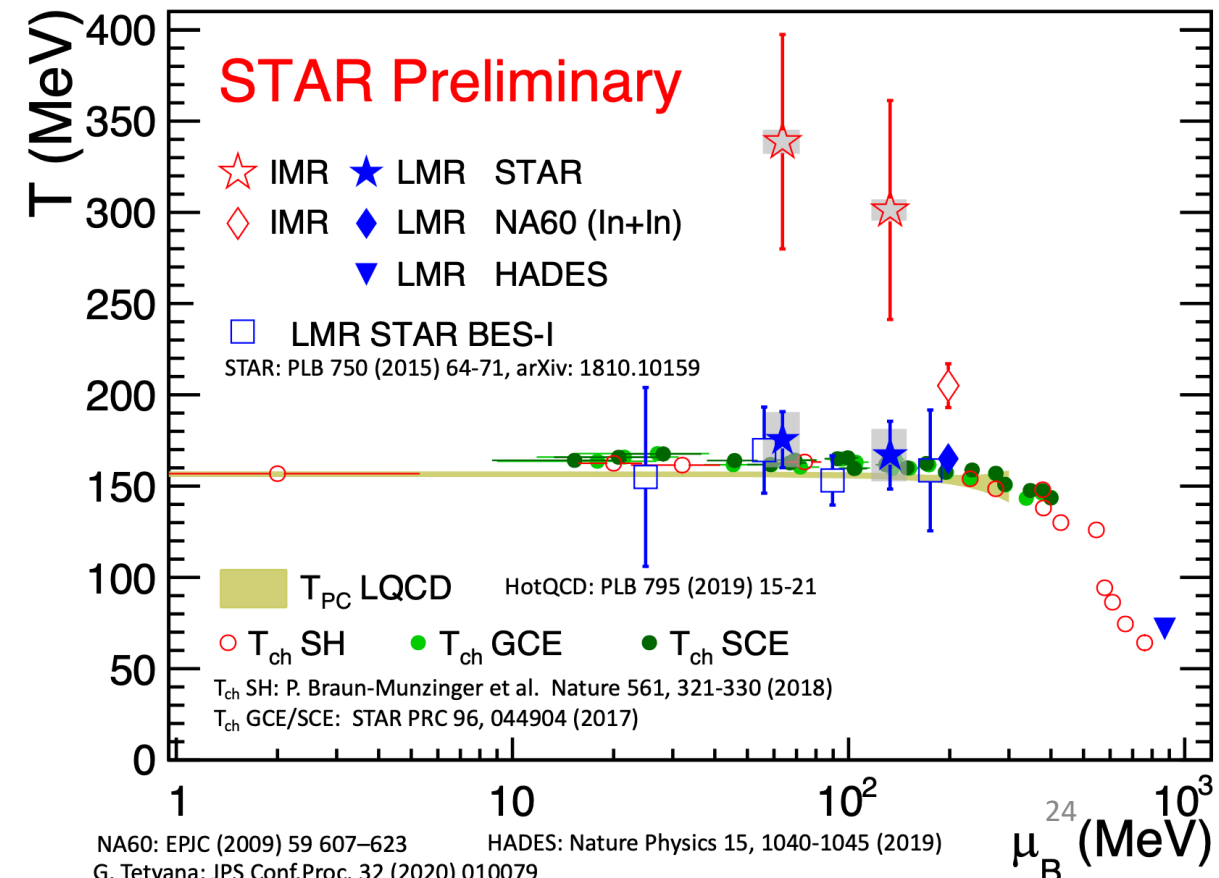
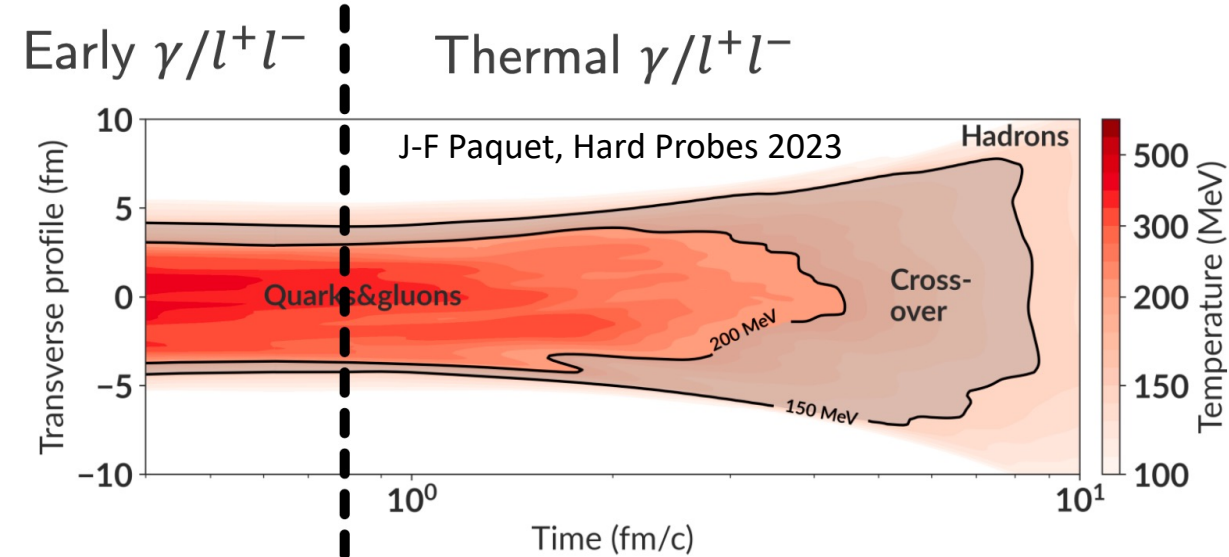
Utilizing penetrating probes, sensitive to the local properties of the emission source, we study

- The phase diagram of QCD
- The plasma temperature and its time evolution
- Medium properties such as shear and bulk viscosity
- Pre-equilibrium dynamics
- Chiral symmetry restoration

Experimentally very challenging due to enormous backgrounds

The STAR BES II program, ALICE in Runs 3 and 4, the future experiments NA60+, CBM, and ALICE 3 with new detector capabilities will provide high-precision measurements.

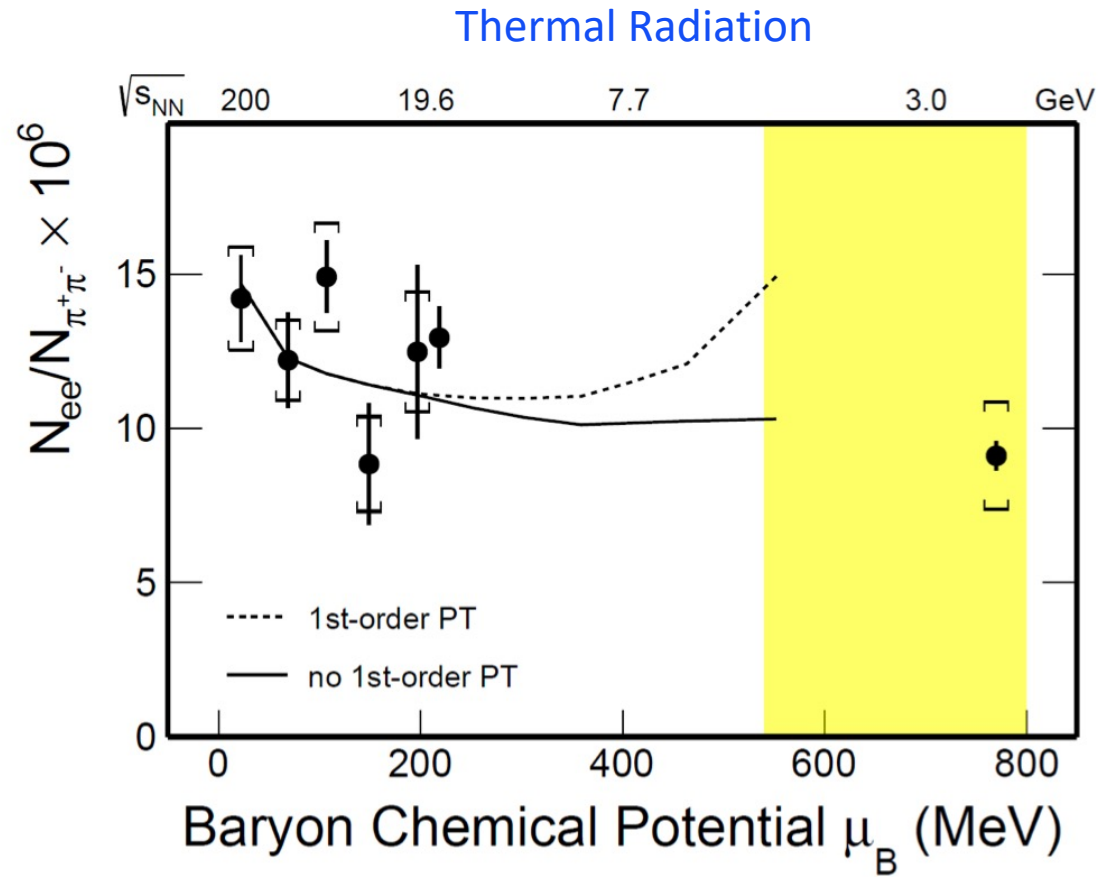
The simultaneous systematic study of soft photons and dileptons, along with soft hadrons and other observables, will provide unparalleled constraints on the properties of deconfined nuclear matter.



NA60: EPJC (2009) 59 607–623
 G. Tetvina: IPS Conf.Proc. 32 (2020) 010079

HADES: Nature Physics 15, 1040-1045 (2019)

Dileptons



Probe first order phase transition

The phases of QCD matter

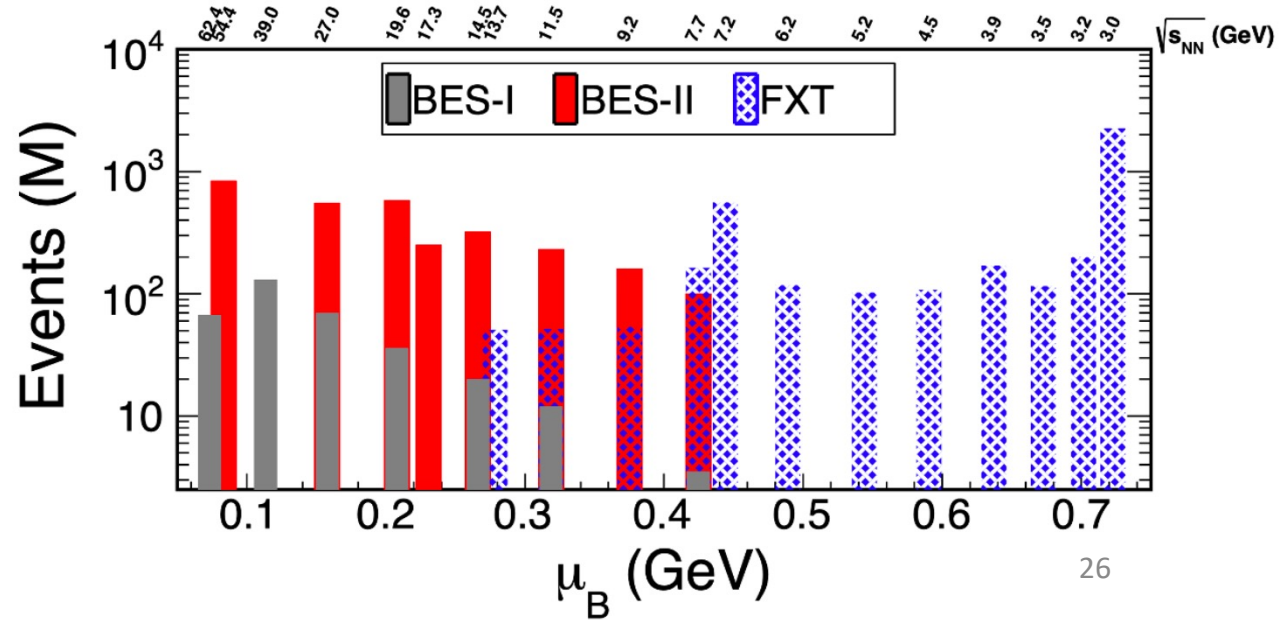
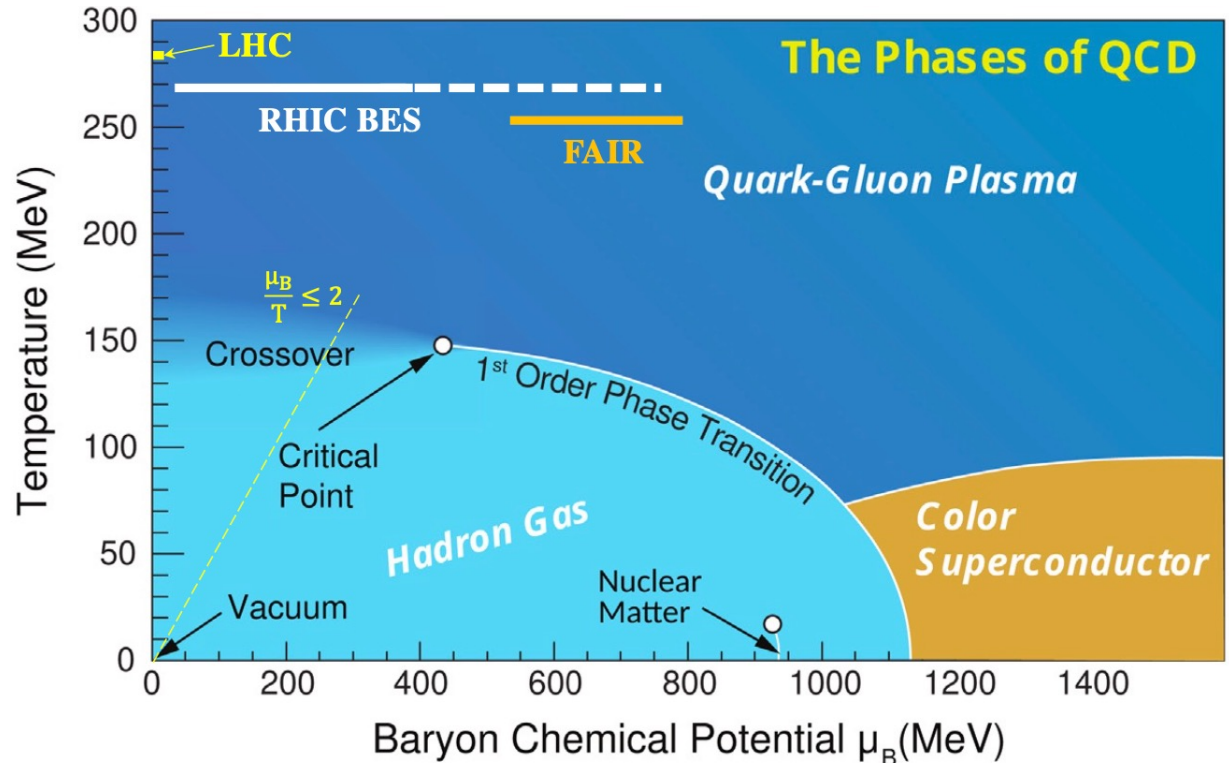
Progress since last LRP:

Lattice QCD: crossover chiral transition at $\mu_B < 2 T$

At top RHIC and LHC energies, measurements consistent with a smooth crossover chiral transition

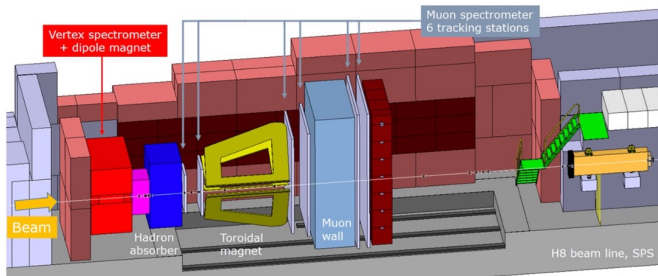
RHIC Beam Energy Scan Phase I (BES-I) measurements imply the QCD critical point, if exists, should be accessible in the center of mass energy region 3-20 GeV

BES-II data taking (energy range 3 - 19.6 GeV) completed in 2021, physics analyses under active pursuit

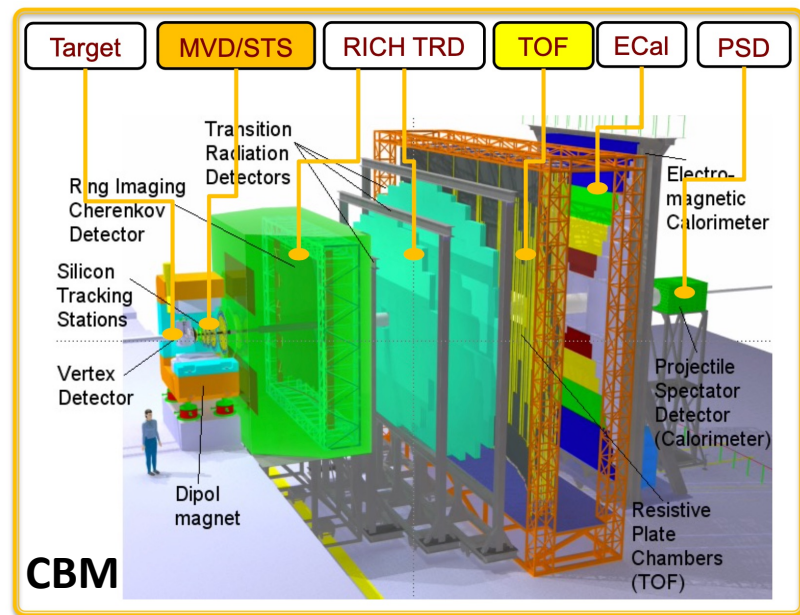
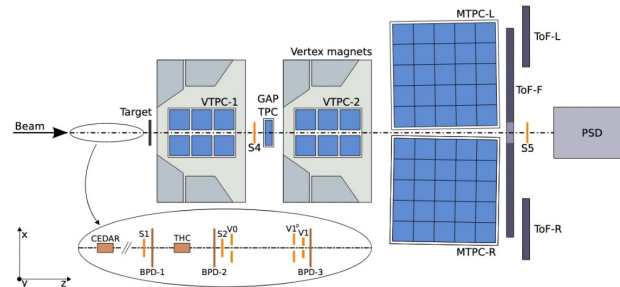


The future

NA60⁺ (2029)

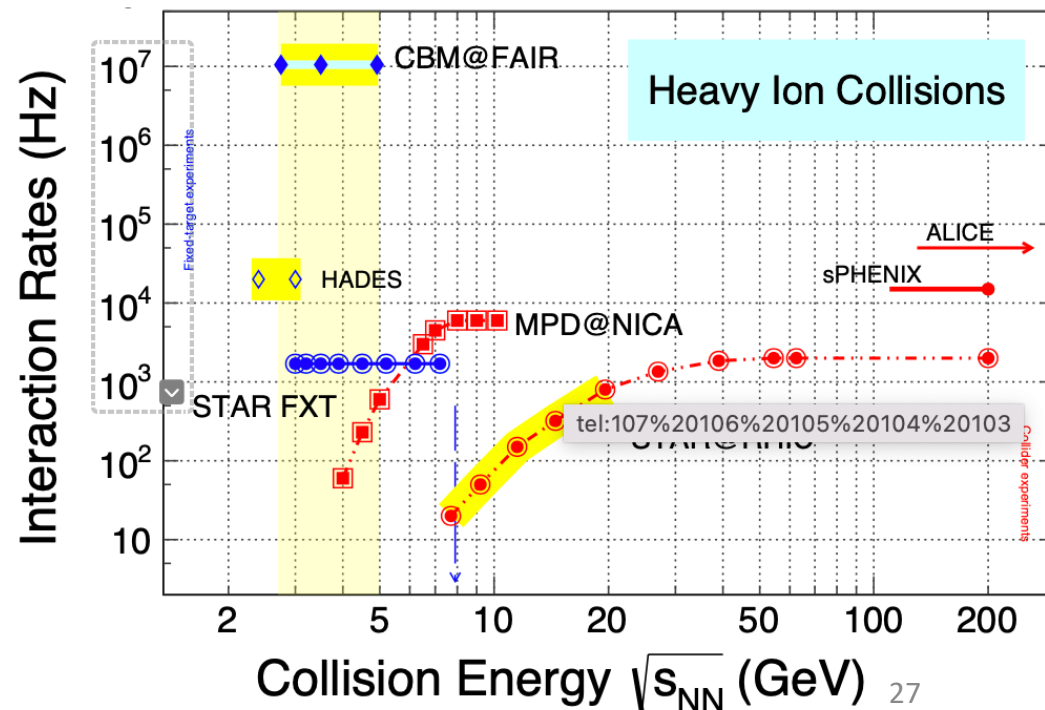


NA61 (2008 - 2027)



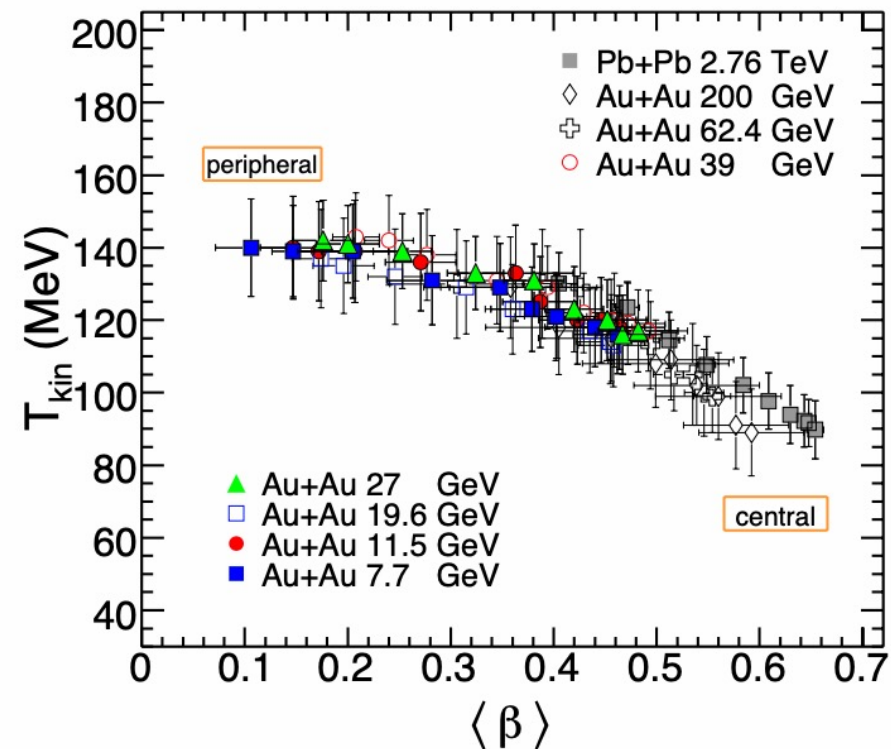
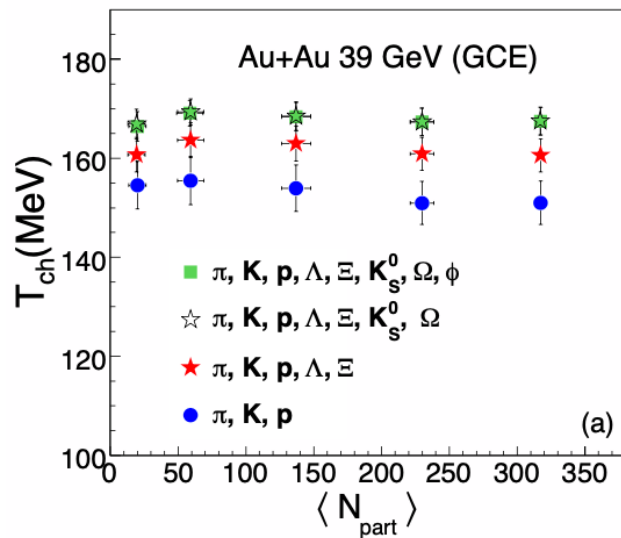
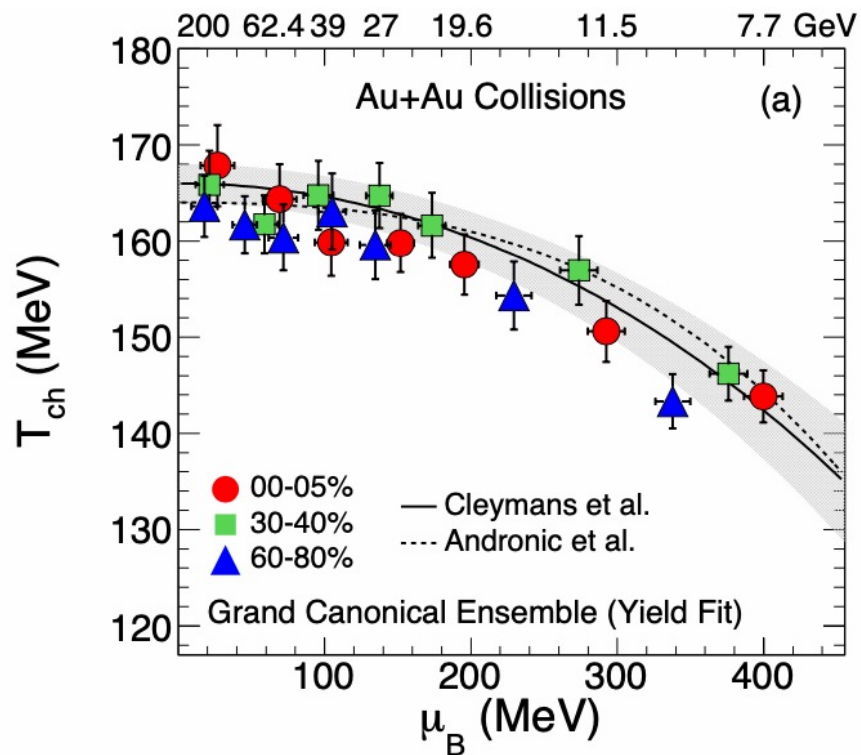
Physics opportunities in the exploration of the QCD phase diagram at high baryon density after the completion of the RHIC BES-II program: NA60+, NA61, CBM, NICA ...

Probe the physics of dense baryon-rich matter and constrain the nuclear equation of state in a regime relevant to binary neutron star mergers and supernovae.



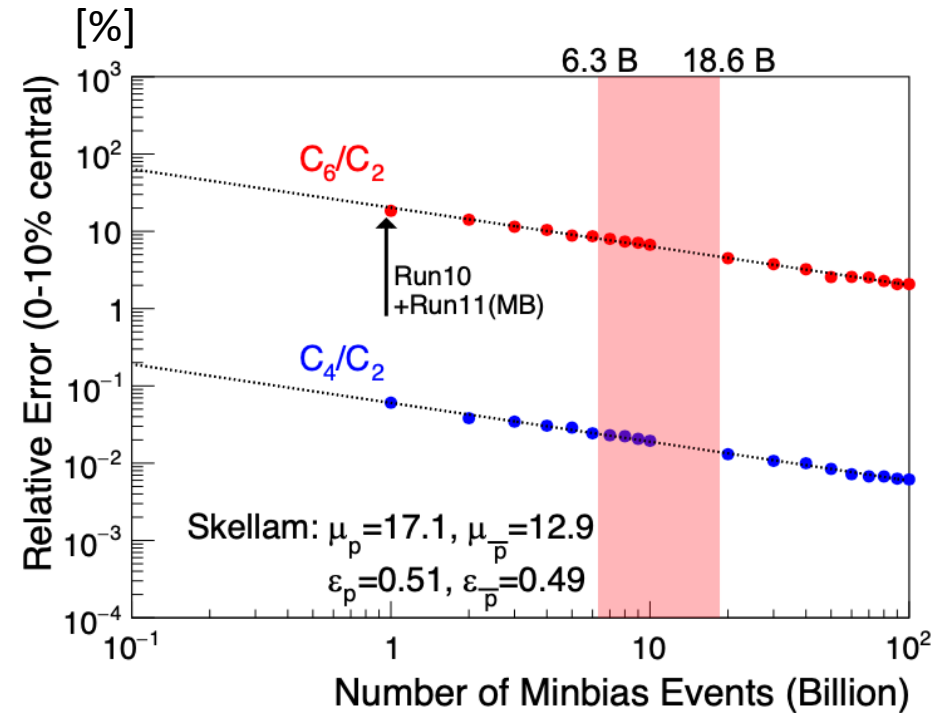
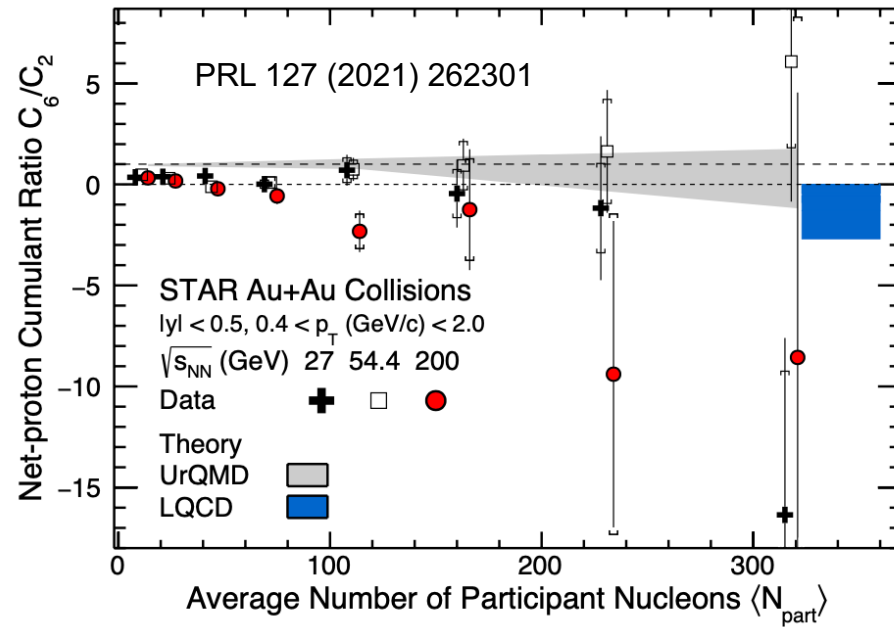
Backup

Freeze out temperatures



Chiral cross-over transition

Improved PID, extended η coverage by iTPC



Lattice QCD predicts a sign change of susceptibility ratio χ_6^B/χ_2^B at T_C

The cumulants of net-proton distribution sensitive to chiral cross over transition at $\mu_B=0$

Observed a hint of a sign change from peripheral to central collisions at 200 GeV

$C_6/C_2 < 0$ at central collisions

High statistics measurements (10% statistical error for C_6/C_2 in central) will pin down the sign change